Chapter

A MECHANISM FOR COMMUNITY-WIDE DETERMINATION OF THE FUNDAMENTAL PHYSICAL CONSTANTS OF QED AND THE STANDARD MODEL

John C. Martens [*] ***and John P. Ralston***
Department of Physics and Astronomy
The University of Kansas, Lawrence, KS, US

Abstract

The values of fundamental physical constants are crucial for testing current theories and their possible extensions. It is not widely appreciated that determining the constants is quite sensitive to how data and theory are selected, and how theoretical and experimental uncertainties are treated. There exists no universal definition of the best procedures or constants. Procedures dedicated to finding constants with the highest possible precision generally select data that confirms the theory. Contrary to perceptions, the theory is not tested at the same level as the uncertainties of fitted parameters. The uncertainties found under a given procedure also cannot reliably constrain parameter variations from different procedures. Determining physical constants cannot consistently be done piecemeal, but needs global fits incorporating the shifting relationships between theory and data. An important example comes from high precision data for muon physics. A circular process has previously excluded

[*] E-mail address: martens@ku.edu.

muonic proton and deuteron charge radius data from global fits to the constants, creating a false perception those data represent a disagreement between data and theory. When the excluded data are included, we find their effects improve the global fit to all constants: And there are many other examples. We claim it is scientifically productive to include generic alternatives in global fits, if only to test sensitivity to their effects. Since all the constants are coupled, it is generally necessary to re-do global fits to place self-consistent limits on alternative theory parameters, or make discovery claims. Yet the procedural universe where QED and Standard Model theory are defined to be exact permits no alternatives. We propose a new mechanism where dependence on data selection, theory, and procedural decision can be explored community-wide. We constructed *Constant Finder* (http://www.constantfinder.org), a comprehensive automated code and user interface available to anyone via the website with the same name. The site allows users to make their own procedural decisions, adjust experimental and theoretical values and uncertainties, and pose alternatives to theory within several global data-fitting frameworks. Anyone interested can determine the fundamental constants on the basis of data, uncertainties, and theory inputs of their choosing.

1. The Present Worldview of Fundamental Constants

The nature of fundamental constants has evolved tremendously. It was possible once to think fundamental physical constants were self-defining experimental quantities not needing a theory. Since the onset of QED, fundamental constants no longer define themselves. Physical constants get their definitions and their meaning from the theory where they are used. Theory was transformed by the emergence of the Standard Model. The definitions of the fundamental constants were transformed again, while the names stayed the same.

The *electron mass* m_e now refers to a parameter in the Dirac sector of the Lagrangian of the Standard Model. Its definition makes no mention of $\vec{F} = m_e\vec{a}$, and nothing about Newtonian physics should appear in the parameter's determination. The *electron charge* e now has three distinctly different definitions. Nothing about the 19th century force on an electron is relevant. When the Dirac Lagrangian is written in one way –as initially done in atomic physics and QED – it appears that e is an independent fundamental parameter. Sommerfeld noticed the dimensionless combination $\alpha = e^2/4\pi\epsilon_0\hbar c$ appearing in perturbation theory. At the time it appeared that all of e, $\hbar$ and c were needed separately. When QED is written a different way, e disappears, and the fine structure constant is revealed as an independent fundamental parameter. Meanwhile the names "electron mass, charge and fine structure constant" tend to be retained in an intellectual perspective developed at Sommerfeld's time or before.

The modern era of high precision measurements has created a new situation in fundamental physics. The main scientific reason to concentrate on high precision constants is to test theory and explore theoretical alternatives. Posing scientific alternatives is not mere speculation: Science exists by posing alternatives. An alternative theory does not change one constant, but generally disrupts the network of relationships involved in the global determination of many constants. Yet this is not generally understood: Most of the time, a new experiment or a new theory variation will deal with one constant that gets attention, as if determining the other constants were independent, and written in stone.

Scientists generally assume that tables of fundamental constants have been determined with extreme objectivity. Yet compiling fundamental constants is a form of data analysis. There are no universal rules for data analysis, while there are sensible guidelines. The actual decisions scientists make depend on the field they happen to inhabit.

Decisions can cause constants to be evaluated on the narrowest possible grounds. Yet dealing with fundamental constants piecemeal leads to inconsistencies. For example, high precision comparisons between theory and experiment for the electron's anomalous magnetic moment are claimed to severely limit alternatives. Yet a change in the theory, either from a new contribution or a change in the calculation, can greatly exceed the nominal uncertainty. One reason is that such a change revises the value of α, which must be re-determined self-consistently. The amount of weight given to such comparison is not a preordained scientific question: It depends on more information than available from the exercise of making a fit.

The relationships between fundamental constants and data is a topic of interest to everyone in physics. The freedom to explore assumptions should be available for everyone to explore. We will discuss a new and open process for exploring fundamental constants. The technology exists to automate the exploration. We have developed an on-line computer code, called the Constant Finder, that allows anyone interested to determine fundamental constants on the basis of data, uncertainties, and theory inputs selected by the user. It is very interesting to find how much depends on judgment and *decisions* that are not widely appreciated.

1.1. Processing Information Is Conditional on Information

Fitting fundamental constants to data is *conditional* upon information available at a given time, and how it is used.

In general a likelihood function $P(data|\theta)$ describes the probability of data given parameters θ. A least-squares fit finding a reasonable value of χ^2 is a typical likelihood, *subject to* assumptions that should be specified. For example, if a good value of χ^2 depends on adjusting theory or experimental uncertainties until a good value is found, the conditions should be divulged.

The likelihood of data, given a parameter, is not actually useful until related to $P(\theta|data)$, *the probability of the parameters* given the data. This sort of probability is subtler than repeating a determination many times and counting frequencies. The importance of prior information and its weight is paramount.

For example, one might have an unshakable faith in the validity of perturbative QED, believing that the higher the order of approximation, the more perfect the theory. Actually theory finds such faith is not justified. Perturbative calculations with Feynman diagrams do not produce a convergent series. The series at best is *asymptotic*. Such a series approaches the true answer as the parameter (coupling constant) goes to zero for a fixed number of terms. The physical limit is different: It uses a fixed coupling, and a variable number of terms. In the physical limit an asymptotic series will begin to *diverge* for a certain number of terms. That is, adding more terms can make the calculation *worse*. Given this information there are reasons to be cautious in interpreting theory calculations. Estimates of theoretical uncertainties are related, but actually a separate issue. Estimates often seem reasonable in advance of calculations. When calculations are later done, theory uncertainties are often found to be underestimated.

Decisions appear at every step. What is better science?: To report the most precise values possible to find for a fundamental constant, while excluding data degrading precision, or to find the most robust value of the constant, using all the information available? It depends on the application. For more than 50 years the US Department of Commerce has contributed to the former aim. According to Ref [3]:

> The Committee on Data for Science and Technology (CODATA) was established in 1966 as an interdisciplinary committee of the International Council of Scientific Unions (now the International Council for Science). Three years later CODATA created the task group on fundamental constants to periodically provide the scientific and technological communities with a self-consistent set of internationally recommended values for the

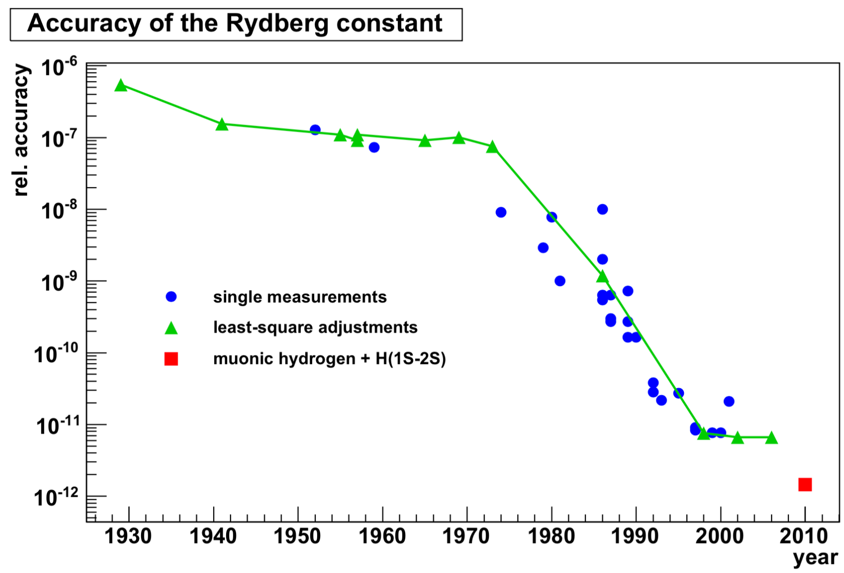

Figure 1. The Rydberg constant is reported very precisely, and also highly contested. The green points show the uncertainty of CODATA global fits versus time, which use the proton charge radius r_p from electron scattering. The red point is an analysis using r_p from muonic hydrogen[1], combined with one experimentally precise $1S2S$ transition of electronic hydrogen. The central value of the red point is also seven standard deviations from the last green one. Analysis and graphics from Ref. [2].

basic constants and conversion factors of physics and chemistry.

It is important to know that the function of CODATA is *not* directed at scientific exploration. CODATA member Savily Karshemboim explains the distinctions [4]:

> Physicists serve as experts only while decisions are made by authorities. The SI system has been created for a legal use and trade rather than for scientific applications...We (physicists) do not care about actual SI definitions partly because we do not consider seriously the legal side of SI...

The charge of CODATA (henceforth abbreviated C) assumes that QED theory is *exact*. This appears repeatedly in C reviews, and the fundamental constants determined on that basis enforce it consistently. It is reiterated when C10 writes "Nevertheless, our main purpose here is not to test physical theory critically, but to obtain 'best' values of the fundamental constants." Perfection requires selection: When discrepancies degrade precision sufficiently, the discrepancies are omitted from the analysis. For example, the measured muon magnetic moment parameter a_μ disagrees with theory by 3.9σ[5]. Retaining it would degrade the uncertainty of α. On page 1549 C10[6] writes that it "has decided to omit the theory of a_μ from the 2010 adjustment," while its experimental value is kept for determining the muon mass most precisely, which causes no discrepancy. But if the data is wrong the muon mass will be wrong. Such decisions are necessary and appropriate for the mission, but one mission cannot fit all purposes.

A different mission statement is found with the collaboration known as the Particle Data Group (PDG). The first *Review of Particle Physics* of 1957 has grown to an annual report that is the top-cited reference in high-energy physics. While the PDG reviews values of physical constants, no particular efforts are made to create final, recommended best values. For example the table listing limits on the photon mass[7] has about 22 values from 22 sources spanning 40 years. The style of the PDG is well suited to research areas where scientists tend to follow and update their own choices from the literature, while assuming that experiments and theory are *not* exact.

1.2. Objectivity Is Difficult: Scheme Dependence Matters

The role of judgment and decisions in determining fundamental constants cannot be overemphasized. Denying it would be tantamount to wanting the "electron mass " or "electron charge" to be defined by 19th century experimental definitions. Theory no longer tolerates circular determinations of fundamental constants by selecting the "best" data. The concept contradicts consistent use of *renormalized* parameters. Just to be clear, the infinities of perturbation theory associated with "renormalization" are a side issue. The procedures got great attention early because *arbitrary conventions* entered. But fundamental constants depend on a theory, and implementing the theory involves arbitrary decisions. Renormalization fundamentally consists of consistently keeping track of decisions fitting data in one circumstance, so they are respected faithfully in another circumstance.

The exact definitions used to determine a set of parameters are intrinsically arbitrary. This is not obvious until one does the work. The procedural conventions are called *scheme dependence.* The fundamental constants as compiled in tables come with multiple forms of scheme dependence that include decisions on methods of fitting, the treatment of experimental and theoretical uncertainties, the selection of observables and data, and more. Somewhere in the list is the scheme dependence of ultraviolet cutoffs. It must be consistent between (say) the non-relativistic conventions of atomic physics and spectroscopy, and the explicitly Lorentz invariant methods used for (say) anomalous magnetic moments. The theorists are competent: They know about scheme dependence. Yet the history of events produced fundamental constants with no mention of ultraviolet scheme dependence, outside the parameters of high energy physics.

Precision experiments also have an element of scheme dependence. Experimentalists must decide what precise signal obtained under what highly particular circumstances from a given apparatus will be reported. Different conventions will yield different results. Don't tell us that every experimental variation produced exactly the same result! Nothing about fundamental constants is carved in stone.

Yet there is currently little overall consensus on the extent to which *procedural dependence* should be reported. For example, some experimental papers awarded immense impact on high precision constants are four-page letters with just a few paragraphs of description, never followed by full-length reviews. Other works may come with exhaustive reviews and many doctoral dissertations providing abundant details. Science is a living thing and quite inconsistent. The irregularity of reporting details undermines the faith that might be given to reported uncertainties. Yet the user of fundamental constants imagines on faith a process that was magnificently objective. On an objective basis no information should be a final authority, and all is a starting point for discussion. Nothing should depend on faith: Anyone interested in the details or alternatives should be free to explore them.

Figure 2 shows the recent history of published determinations of α[8] as a function of time. For each jth determination, the y-axis shows the subsequent difference $(\alpha_{j+1} - \alpha_j)/\bar{\Delta}\alpha_j$, where the reported uncertainties are $\sigma_{\alpha j}$, with the average $\bar{\Delta}\alpha_j = \sigma_{\alpha j+1} + \sigma_{\alpha j+1}$. Error bars are $10^3\bar{\Delta}\alpha_j$. The reasons for the fluctuations are discussed in Section 4.3.

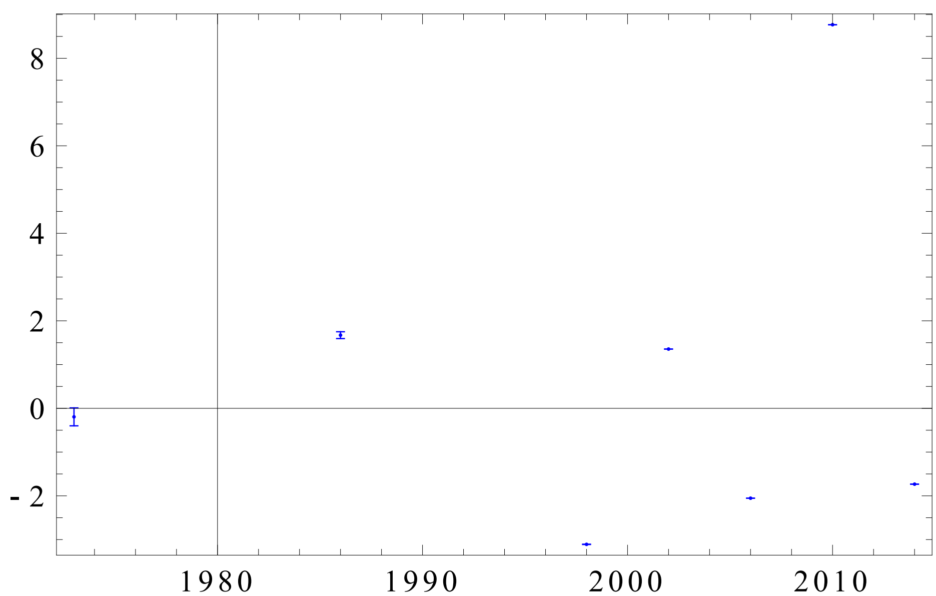

Figure 2. Time dependence of determinations of the fine structure constant [8]. For each jth determination in the year shown, the y-axis shows the subsequent difference $(\alpha_{j+1} - \alpha_j)/\bar{\Delta}\alpha_j$, where the reported uncertainties are $\sigma_{\alpha j}$, with the average $\bar{\Delta}\alpha_j = (\sigma_{\alpha j+1} + \sigma_{\alpha j+1})/2$. Error bars are $10^3\bar{\Delta}\alpha_j$.

1.3. The Need for a Vehicle for Discussion

At the present time the community has little or no mechanism encouraging discussion. Consider the electron and muon anomalous moment parameter $a_e = (g_e - 2)/2$, where g_e is the Landè g-factor. What are the effects on the value and uncertainty of α upon doubling the parameter's experimental error? Experimentalists at the Large Hadron Collider have generally agreed on a criterion of five standard deviations to announce a discovery. We mentioned the Brookhaven data for the muon anomalous moment disagrees with calculations by 3.9 units of the estimated uncertainty[5]. But on what basis is the statement of a 3.9σ disagreement made? Since 3σ discrepancies are not so rare in science, is the discrepancy meaningful? What if the uncertainty in α is adjusted one way, and the experimental measurement uncertainty adjusted another way: Will it be impossible *in principle* to reconcile the data? Such questions should not be considered idle speculation. Testing the Standard Model is very important. The scientific method involves posing alternatives, where the size of error bars should be just as subject to challenge as anything else.

Table 1. A few examples of best fits to fundamental constants using the Constant Finder when data is selectively removed. Parentheses list the standard uncertainties. Removing a_e has negligible effect. Retaining a_μ while doubling its experimental uncertainty ($\star$) while removing a_e and λ_e has negligible effect. It does revise the central value of α significantly (Section 3.3). Removing a_μ altogether reduces χ^2 by nearly 16 units. Table 6 shows many other examples.

Omit	χ^2_{tot}	dof
$none$	27.5	17
μH	25.1	16
μD	27.3	16
a_e	27.3	16
$a_e,\, \lambda_e; \star$	27.5	15
a_μ	11.8	16

Since each specialized group excels within its own sphere, many physicists assume each constant is determined by a group that cares about it. There is a complacency to let the specialists settle their own concerns. Some will be amused or interested to hear of the number of digits known for α or the Rydberg constant R_∞, without caring about it further. Yet a crisis among the fundamental constants has come about and been hidden in plain sight. Physics *does not have a generally accepted theory* that explains all high precision data. Rumors that the Standard Model is in 100% accord with all data come from rejecting some of the data. See Table 1 extracted from Table 6 in Section 3.3, which has the details. The table shows how the χ^2 statistic of a basic global fit changes when the data are included, or removed. Removing the muon anomalous moment parameter a_μ improves χ^2 by nearly 16 units, which is usually considered significant. However removing a_μ makes $\chi^2/dof \to 11.8/16$, which is smaller than expected statistically, and potentially as significant as finding χ^2 too big. If one wants to keep a_μ the table shows one way to do it.

The electron anomalous moment parameter a_e is often reported to be decisive. Yet removing it causes an entirely *negligible* change in χ^2. It is sometimes reported that muonic hydrogen and deuterium data disagree with the Standard Model, which is called the "proton size" problem. The table shows the change in χ^2 is not significant when removing the μH, μD data. The perception of an inconsistency comes partly from decisions excluding selected muonic data so as to maintain continuity in the value of R_∞ compared to its previously determined value.

Thus the "absolute best determinations" of α, R_∞, the anomalous magnetic moments of the electron and muon, the proton's charge radius r_p, its mass and the electron mass, are *not* mutually consistent with the QED theory where they are evaluated. Yet this statement depends critically on the central values and uncertainties of the data used in the analysis. It also depends on the system for evaluating information, which over time developed a gap in the scientific method.

The gap in fundamental constants has allowed no mechanism for an informed physicist to personally investigate the science behind the constants. Physicists should be allowed to know the consequences that input assumptions have on outputs. Instead of using (say) 21 transitions of atomic hydrogen or deuterium with certain reported uncertainties, one can use five, or one. The consequences of retaining one most precise experimental point –whose theoretical uncertainty is thousands of times larger than the experimental one– can be explored by adjusting the inputs, and examining the outputs. The electron and muon anomalous moments can be varied in value and uncertainties, to explore the global consequences on, say, the Rydberg constant. When data or assumptions change, the Constant Finder code will reflect the consequences in a few milliseconds. The code has been validated by producing it in two independent versions, on two different machines, and exhaustively comparing it to previous work. So far this code is a prototype with limited scope that serves as a proof of principle. In the future, however, more ambitious and user-friendly versions can fill the gap in the needs of working physicists.

Section III reviews the online code and provides examples of how it works. Section II provides background on the *presently configured* logical relations between the values of the fundamental constants. That Section will demonstrate the inherently global nature of fits to the constants. Unless assumptions are so mild as to have no consequences, it is *almost never consistent* to introduce one updated datum, or revise one theory element, and maintain self consistency at the level given by published tables. For example, the relationships between QED and the constants are such that the theory is not tested at the highest precision that is reported. The relationships are not definitively tested by the *next most stringent* data items. The tests of theory and experiment come in the overall consistency of global fits with *many* potentially subjective decisions. Our accomplishment is to democratize the freedom to make procedural decisions, *given* published information, which had previously existed only for specialists in the field.

2. Background on Data and Procedures

A Lagrangian field theory will have one parameter for every term not predicted by a symmetry. The Standard Model including neutrino masses has 26 parameters, which consist of 20 quark and lepton masses and mixing angles, three gauge coupling constants, two parameters of the Higgs sector, and the speed of light c.

Some authors include a strong CP violating parameter θ_{QCD}, whose interpretation is ambiguous, while most omit c by choosing units where $c = 1$. However the speed of light is an observable parameter of the universe. Regardless of the units, all agree there exists a particular upper limit on the speed of massive objects in this universe[1]. The computational convenience of choosing

[1] One can also define separate fundamental length and time scales, with e.g. the size of the hydrogen atom and the frequency of a muonic atom.

$c = 1$, and the technological convenience of defining the length unit with a reference value for c, happen to be completely independent issues. Yet due to the arbitrariness of units the number for c is not informative in the current theory.

Table 2. Experimental data used in default global fits of this paper. Standard Model physics is assumed. Data from Refs. [9, 10, 11, 12, 5, 2, 13, 14].

Experimental datum [units]	Experimental value	σ_{expt}
$\nu_H(2S1/2 - 8S1/2)$ [Hz]	$7.70649350012000 \times 10^{14}$	8600
$\nu_H(2S1/2 - 8D3/2)$ [Hz]	$7.70649504450000 \times 10^{14}$	8300
$\nu_H(2S1/2 - 8D5/2)$ [Hz]	$7.70649561584200 \times 10^{14}$	6400
$\nu_H(2S1/2 - 12D3/2)$ [Hz]	$7.99191710472700 \times 10^{14}$	9400
$\nu_H(2S1/2 - 12D5/2)$ [Hz]	$7.99191727403700 \times 10^{14}$	7000
$\nu_H(2P1/2 - 2S1/2)$ [Hz]	$1.05784500000000 \times 10^{9}$	9000
$\nu_H(2S1/2 - 2P3/2)$ [Hz]	9911200000	12000
$\nu_H(2P1/2 - 2S1/2)$ [Hz]	1057862000	20000
$\nu_D(2S1/2 - 8S1/2)$ [Hz]	$7.708590412457 \times 10^{14}$	6900
$\nu_D(2S1/2 - 8D3/2)$ [Hz]	$7.708591957018 \times 10^{14}$	6300
$\nu_D(2S1/2 - 8D5/2)$ [Hz]	$7.708592528495 \times 10^{14}$	5900
$\nu_D(2S1/2 - 12D3/2)$ [Hz]	$7.99409168038 \times 10^{14}$	8600
$\nu_D(2S1/2 - 12D5/2)$ [Hz]	$7.994091849668 \times 10^{14}$	6800
$\nu_D(2P1/2 - 2S1/2)$ [Hz]	1059280000	60000
$\nu_D(2S1/2 - 2P3/2)$ [Hz]	9912610000	300000
$\nu_D(2P1/2 - 2S1/2)$ [Hz]	1059280000	60000
a_e	0.00115965218072	2.8×10^{-13}
a_μ	0.00116592089	6.3×10^{-10}
$\Delta E_{LS}(\mu H)$ [meV]	202.3706	0.0023
$\Delta E_{LS}(\mu D)$ [meV]	202.8785	20.0034
λ_e [m]$/10^{-12}$	2.4263102367	1.1×10^{-9}

Nowadays the fundamental constants are partitioned into those used for high precision work and the rest. High precision work typically involves the constants listed in Table 2. In most of the discussion here we assume fitting Standard Model theory with parameters $\theta_j = (\alpha,\, R_\infty,\, r_p)$, along with the deuteron charge radius analog r_d when spectroscopic deuterium data is included. The choice of what data to include and how to incorporate theory uncertainties is quite important.

Notice that not all experimental inputs are known to great precision: The value of the proton and deuteron charge radii, in particular, are controversial at the few-percent level. For reasons we will explain those values and uncertainties are highly correlated with R_∞. The Rydberg also depends sensitively on α and the electron Compton scale[2] $\lambda_e = h/m_e c$. Ultimately c/λ_e is the fundamental frequency scale dominating the spectra of atomic physics. Finally α is exquisitely sensitive to the electron anomalous moment parameter a_e. It is not self-consistent to "test QED" by comparing α and calculations of a_e. The exercise itself fits a parameter while testing nothing: The actual tests involve other quantities, which are inextricably linked in a global network.

2.1. Choosing a Global Analysis

There are three basic levels to a conventional least-squares fit. The most basic one fits a conventional χ^2 statistic

$$\chi^2 = \sum_j \frac{(d_j - t_j(\theta_\ell))^2}{\sigma_j^2}. \tag{1}$$

Here d_j and t_j stand for the jth instances of data and theory values depending on parameters θ_ℓ. The symbol σ_j stands for the experimental uncertainty. It is easy to show that χ^2 is the log-likelihood of a product of Gaussian distributions with argument $(d_j - t_j(\theta_\ell)$ and width parameters σ_j. The maximum likelihood fit coincides with minimizing χ^2.

The next most elaborate procedure, sometimes called "χ^2 with pull", introduces additive offsets δ_j whose effects are regulated by additional terms:

$$\chi_\delta^2 = \sum_j \frac{(d_j - t_j(\theta_\ell) - \delta_j)^2}{\sigma_j^2} + \sum_j \frac{(\delta_j - \bar{\delta}_j)^2}{\sigma_{\delta j}^2}. \tag{2}$$

This represents the likelihood incorporating a model of prior information about the data and theory. To be specific, let the distribution of data given parameters

[2]The Compton wavelength or "quantum of circulation" refer to equivalent quantities. Neither m_e nor h has been determined with the precision typically needed for precision atomic physics. However their uncertainties are 100% correlated, and cancel in m_e/h.

$f(d_j|\theta_\ell,\,\delta_j) = exp(-(d_j - t_j(\theta_\ell) - \delta_j)^2/\sigma_j^2$, up to a normalization. Let δ_j be distributed like $f(\delta_j) = exp(-(\delta_j - \bar{\delta}_j)^2/\sigma_{\delta-j}^2)$. Then the log-likelihood $\mathcal{L}$ of the parameters given the data is

$$\mathcal{L} = log \prod_j f(d_j|\theta_\ell, \delta_j) f(\delta_j) = \sum_j log(f(d_j|\theta_\ell, \delta_j)) + log(f(\delta_j)),$$

which gives Eq. 2. Integrating out the δ_j parameters in such a distribution effectively replaces $\sigma_j^2 \rightarrow \sigma_j^2 + \sigma_{\delta j}^2$ in the denominator of Eq. 1, equivalent to "adding errors in quadrature."

The additive offsets serve more than one purpose. They are a common way to represent theory uncertainties, including un-calculated terms of the theory (which despite perceptions of QED, are not all known at the same order of approximation). The offsets can also signal potential issues with data. When Eq. 2 is minimized directly, the physical parameters and additive offsets δ_j are fit at the same time, creating a sort of microscope into the fitting process.

However the process can be extremely sensitive to the widths $\sigma_{\delta j}$. By inspection each term from the theory can be fit trivially when δ_j are large enough, which is always possible with sufficiently large $\sigma_{\delta j}$. That creates an opportunity to tune final results with potentially subjective nuisance parameters. It is neither wrong nor dishonest, but represents a Bayesian element that always exists in data analysis. However if outputs are discovered to be very sensitive to procedural decisions that information should be divulged. We have found that arbitrary (but also, justifiable) procedural decisions often significantly affect the fit results, which led us to the publicly usable code concept.

The next most elaborate analysis will introduce correlation parameters into the Gaussians. Either this produces minor changes in outcomes, or major ones. When many correlation parameters are introduced the possibility for sensitivity to procedural decisions is greatly increased. If major effects from such decisions are found, it increases the need to understand and report the reasons for them. All three methods can be used in any combination in our online code, as detailed in Section III.

2.1.1. Allowing a Theoretical Alternative

The history of physics shows that progress requires comparing alternatives. In early celestial mechanics the gravitational potential was modified with one parameter to $1/r^{1+\epsilon}$, simply to have an alternative. Later General Relativity provided a more complete theory, at first considered to be an alternative to Newtonian gravity. Then high-precision discrepancies of the older theory, such as the precession of Mercury's perihelion, became consistency tests of the new theory. Permitting almost any alternative model often improves data analysis for rather subtle reasons. The solution space of physical parameters can dramatically change by adding dimensions. Changing $1/r \to 1/r^{1+\epsilon}$ might generate a much better *signal* of a discrepancy than repeatedly fitting $1/r$ physics with better and better data. A signal probably does not indicate "new physics" and might have a thousand reasons. It is simply unreasonable *to forbid looking* for new signals.

With this in mind, our code is built to allow modifying formulas for each term. It is common but not mandatory to express an alternative in terms of a new interaction. We follow suit here, introducing for definiteness a "no-name" particle X, with coupling α_X and mass m_X [15]. For example, the Yukawa potential of a scalar interaction at radius r is

$$V_X = \alpha_X \frac{e^{-m_X r}}{4\pi r}$$

In first order perturbation theory the energy shift of a hydrogenic bound state $\psi_{n\ell}$ is[3]

$$\Delta E_n(X) = \int d^3x \, \alpha_X \frac{e^{-m_X r}}{4\pi r} \psi_{n\ell}^2(r) = 8.11 \times 10^{20} \cdot \frac{\alpha_\chi \alpha^3}{n^3 m_\chi^2} \, \text{Hz}. \tag{3}$$

So long as α_X/m_X^2 is small enough, such a first-order term will contribute to the Lamb shift at a level comparable to the smallest observable terms of QED. No elaborate, top-down theoretical superstructure is necessary to explore data fits. It is sufficient to modify formulas in terms of additional parameters denoted θ_X. Examples are given in Section 3.4.

2.1.2. Making a Fit

Our illustrations show how to determine α, R_∞ and proton and deuteron charge radius parameters r_p, r_d with high precision data. Symbol a_e stands for the electron's anomalous moment parameter ("anomaly"), f_{eH}, f_{eD} stand for hydrogen

[3]Counting on our hands, we expect $\Delta E \sim (\alpha m_e/n)^3(\alpha_\chi)(1/m_\chi)^2$, where the first factor comes from the normalization of $\psi_{n\ell}$ and the second factor from the Yukawa, while the third factor, from the integral, is needed to cancel two of the powers of m_e in the first term so that ΔE has the correct dimensions.

and deuterium transition frequencies, $f_{\mu H}$ and $f_{\mu D}$ stand for muonic Lamb shift measurements in hydrogen and deuterium, and m_e comes from atomic recoil and mass ratio experiments. Symbol θ_X stands for any additional parameters. A basic fit is expressed with

$$\chi^2 = \frac{(a_e^{exp} - a_e^{theory}(\alpha,\, \theta_X))^2}{\sigma^2(a_e)} + \frac{(a_\mu^{exp} - a_\mu^{theory}(\alpha,\, \theta_X))^2}{\sigma^2(a_\mu)}$$

$$+ \sum_j^{N_H} \frac{(\Delta f_{eH,j}^{exp} - \Delta f_{eH,j}^{theory}(\alpha,\, R_\infty,\, r_p,\, \theta_X))^2}{\sigma^2(\Delta f_{eH})} + \sum_j^{N_D} \frac{(\Delta f_{eD,j}^{exp} - \Delta f_{eD,j}^{theory}(\alpha,\, R_\infty,\, r_d,\, \theta_X))^2}{\sigma^2(\Delta f_{eD})}$$

$$+ \frac{(\Delta f_{\mu H}^{exp} - \Delta f_{\mu H}^{theory}(r_p,\, \theta_X))^2}{\sigma^2(\Delta f_{\mu H})} + \frac{(\Delta f_{\mu D}^{exp} - \Delta f_{\mu D}^{theory}(r_d,\, \theta_X))^2}{\sigma^2(\Delta f_{\mu D})}$$
$$+ \frac{(4\pi c R_\infty/\alpha^2 - (m_e/h)^{exp})^2}{\sigma^2(m_e/h)} \tag{4}$$

The terms in the order shown will be called $\chi^2(a_e)$, $\chi^2(a_\mu)$, and so on. The parameters we typically vary are displayed explicitly in the expression above, while others whose variations are safely suppressed are set to reference values given on the website.

2.2. Example Parameter: The Fine Structure Constant α

Making independent fits of fundamental constants demands studying the details of the theory and experiments determining them. The study is rewarding and guides decisions. We have provided an extensive Appendix with information on a number of fundamental constants. It appears at the end so we can move more quickly to our main topic, the Constant Finder website. For illustration we here provide background information on one constant known for a century as α.

The fine structure constant α is often introduced in perturbation theory, but actually emerges non-perturbatively and at a very elementary level of quantum mechanics. The Schrödingerequation for the hydrogen atom is

$$\imath\hbar\frac{\partial\psi}{\partial t} = -\frac{\hbar^2}{2m_{MKS}}\vec{\nabla}^2\psi - \frac{e_{MKS}^2}{4\pi\epsilon_0 r}\psi; \imath\frac{\partial\psi}{\partial t}$$

$$= -\frac{\hbar}{2m_{MKS}}\vec{\nabla}^2\psi - \frac{e_{MKS}^2}{4\pi\epsilon_0\hbar r}\psi = -\frac{2\pi\lambda_e c}{2}\vec{\nabla}^2\psi - \frac{\alpha c}{r}.$$

The eigenvalues of the second line have units of frequency, illustrating how easily Planck's constant (which has unacceptably large uncertainties) is bypassed in atomic spectroscopy. By inspection α is dimensionless, and takes the same value in natural units as in the MKS convention.

At a more advanced level, the electromagnetic vector potential of QED is coupled to matter by the Dirac Lagrangian $\bar{\psi}(\imath\partial_\mu - qA_\mu)\gamma^\mu\psi$, where $A_\mu = e\tilde{A}_\mu$ and $q = 1$ for an electron. Using A_μ for the field, the Maxwell term transforms $-\tilde{F}_{\mu\nu}\tilde{F}^{\mu\nu}/4 = -F_{\mu\nu}F^{\mu\nu}/(4e^2)$, where $F_{\mu\nu} = \partial_\mu A_\nu - p_\nu A_\mu$. This shows e is not a separately observable constant, while $\alpha = e^2/4\pi$ is observable. The elementary reason for this is the fact that it takes a charge to observe a charge: Products of charges appear in Coulomb's Law, for example.

The general pattern of precision measurements is that quantities tied to MKS standards are determined at much lower precision than the dimensionless α or quantities related to frequency or length (via crystallography). The Josephson constant $K_J = 2e_{MKS}/h_{MKS}$ and the von Klitzing constant $R_K = h_{MKS}/e^2_{MKS}$ have often been candidates for measuring α. Yet when the analysis is properly arranged the expression $\alpha_{MKS} = e^2_{MKS}/4\pi\epsilon_{0\,MKS}\hbar_{MKS}c$ does not define the fine structure constant. When α is independent, it defines

$$e^2_{MKS}/\epsilon_{0\,MKS}\hbar_{MKS} \equiv 4\pi\alpha.$$

The fact that α is independently observable is clear from theory, which has evolved since α_{MKS} was first defined, to the extent that α_{MKS} now defines e_{MKS} and not the other way around. Take the prediction of the electron anomalous moment parameter $a_e \sim \alpha/2\pi$: A ratio of frequencies observed for electrons in a magnetic field determines a_e with no reference to any MKS units. The improved definition leads to defining $e \equiv \sqrt{4\pi\alpha}$ with relative uncertainty $u_r(e) = u_r(\alpha)/2$. To order of magnitude $u_r(e) \sim 10^{-2}u_r(e_{MKS})$. The measurement of e_{MKS} on the other hand is difficult because it cannot avoid introducing the artifact called the $kilogram$, which degrades precision. The difference between definitions is obscured when the historical MKS definition is made early and not later corrected. Traditionally published tables choose to define the electron charge as e_{MKS}, whose uncertainty is correlated directly with $\hbar_{MKS}$, which is discussed further in Section 4.1.

For many years the precision of experiments measuring a_e so eclipsed other experiments that setting theory $\equiv$ data created a de-facto determination of α and its uncertainties. The literature shows that each new measurement of a_e and each new calculation came with a self-contained announcement for α. Yet those determinations have been almost universally misinterpreted as *tests* of QED at the same level of precision. Fitting one parameter to one theory tests nothing. The associated uncertainty also has no information about the non-trivial comparisons and uncertainties with the entire universe of data where tests are made. The history of the determinations of α is an excellent place to begin learning about the procedural dependence of data and theory selection and its consequences. More on this topic appears in Section 4.3, and (to repeat) Section 4 provides background information on a number of other physical constants.

3. The Constant Finder Code and Website

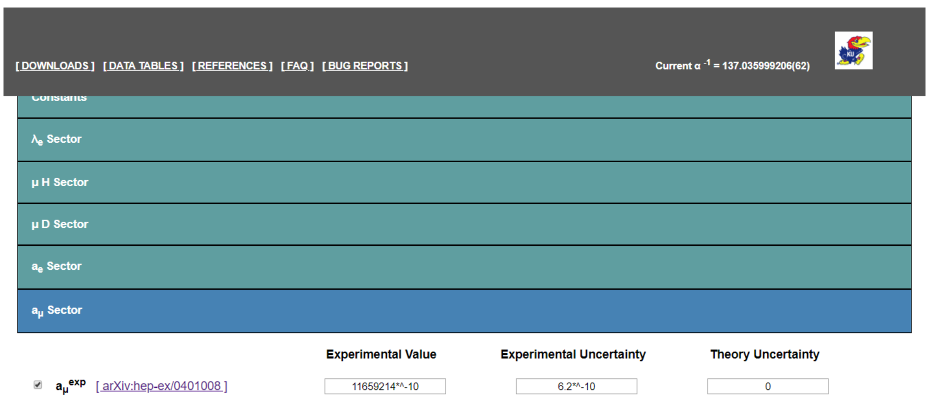

Figure 3. View of the Input Data section of the Constant Finder site. Default values for the experimental value, experimental uncertainty, and theoretical uncertainty of the a_μ datum are shown. Those values can be adjusted by the user via the textboxes shown, or hidden from view via a collapsible menu.

In this section we give step-by-step illustrations of sample analyses which can be explored with the Constant Finder site.

3.1. The Constant Finder Concept

Constant Finder uses webMathematica [16] to perform least-squares global fits to fundamental constants on the basis of user-selected data, uncertainties, and theory formulas. Users can select default methods, data and parameters, or insert their own choices. A simple graphics interface allows users to define the details of a fitting statistic χ^2, including or omitting such features as additive constants (pull parameters). Results can be printed in-browser or exported as a pdf file or Mathematica notebook. Besides exporting results, users can also export a record of inputs and intermediate formulas generated in the analysis, such as the specific form of the χ^2-function, which allow for easy creation of graphics and tables offline.

A separate section of the website is reserved for posing alternatives. These alternatives are nominally new physics scenarios, but they do not by themselves, in any eventuality, imply physics beyond the Standard Model (BSM). Anything can be explored: The code does not depend on any model, nor its internal consistency. Instead, the code will accept corrections to standard theory of any kind, treating new parameters as new fundamental constants to be determined globally with Standard Model constants. In case there are degeneracies or indeterminacy in the formulation of the alternative it will usually be signaled automatically in the outputs.

The site is designed to give the user maximum flexibility to test alternatives. For the simplest applications, it takes only seconds to select inputs and generate results. Every effort has been made to maintain the user's independence in analysis decisions and details of fitting. We will limit illustrations to typical examples with typical assumptions. To begin making your own fundamental constants, follow the procedure below.

1. **Navigate to http://www.constantfinder.org.**
2. **Select the type of fit.**
   Select a chi-squared fit method via radio buttons. Choose among built-in options, such as adding theory uncertainties in quadrature to experimental ones, or a chi-squared fit with pull parameters as in Eq. 2. Customize the fitting statistic if desired.
3. **Select the input data.**
   Input data stored on the site is organized by "sector", such as masses, anomalous moments, spectroscopy, etc. Users select a given datum via a checkbox. Each datum consists of an experimental value, an experimental error, a citation to the experiment, and, depending on the fit-type, a theory error or pull parameter error. Default values are generated in an editable textbox. For convenience the experimental values and experimental errors

default to published values, theory errors to zero, and pull parameter errors to the published value of the experimental error. Users have total freedom to insert any input values desired. Users also have the option to add new data to each sector. Figure 3 shows a screenshot of this portion of the site.

4. **The Model Alternative Option**
Radio buttons allow users to introduce and explore alternatives. If an alternative option is selected, default contributions are instantiated on the site, sector by sector, via three editable textboxes. The textboxes specify the formula encoding the sector-specific contribution to chi-squared, the new parameters to be fit, and any constants not defined internally. The format is defined on the website and repeated in more than one way to avoid errors. For example, the alternative muon's anomalous moment parameter a_μ defaults to $a_{mu}^{SM} + a_\mu^{new}$, where SM stands for Standard Model and new stands for a term revising it. Users specify the formula for a_μ^{new} by typing the formula in the box. Default formulas (discussed in Sections 4.3 and 4.4) generated from a generic no-name boson (Model-X) serve as examples to keep formatting consistent.

5. **Select how to print the results.**
Users can print results in the browser window, as a pdf file, or as a Mathematica notebook using one of three buttons on the site. Results printed in the browser or as a pdf give an overview of the fit, and include the fitted values for all fit parameters, the chi-squared budget for the fit, and the covariance matrix. In addition, contour plots of all possible two-dimensional correlations between fit parameters are generated by default: see e.g. Figs. 8, 9.
The Mathematica notebook gives users great freedom to explore. Any quantity defined in the analysis exists in a Mathematica-readable form, and can be exported for subsequent use. For example, the chi-squared function specific to the front-end inputs exists in symbolic form, and can be exported for use off-line. The tables and figures in this section were generated using Mathematica notebooks generated on the site.

3.2. Input Data and Consistency Checks

We notionally divide experimental data into seven sectors, for convenience. The defaults are as indicated in Eq. 4: An eH sector, consisting of electronic hydrogen transition frequencies; An eD sector, consisting of electronic deuterium

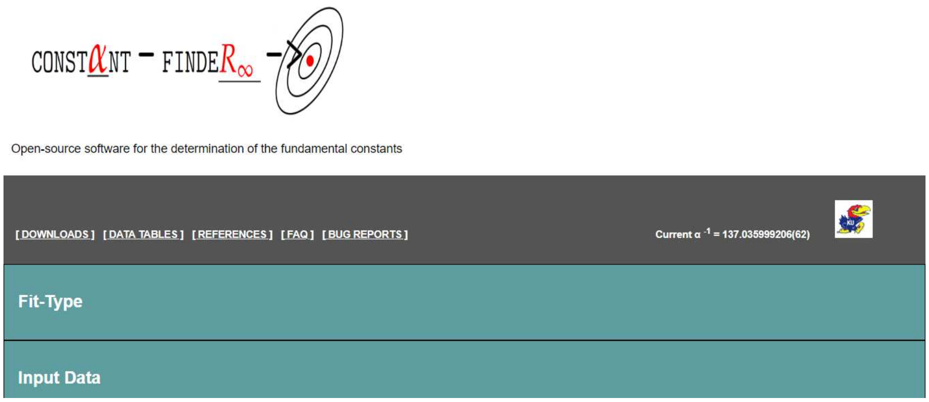

Figure 4. View of the Constant Finder site upon loading. The gray header links to other pages within the site, and remains at the top of the page on scrolling. Users specify inputs via collapsible menus. (Fit-type and Input Data menus are shown.) In this example the value of α^{-1} is adjusted automatically on the basis of the current inputs, showing the effects of decisions as they are executed.

transition frequencies; An a_e sector, consisting of the experimental value of the electron anomalous magnetic moment; An a_μ sector, consisting of the experimental value of the muon anomalous magnetic moment; A μH sector, consisting of the measured Lamb shift in muonic hydrogen; A μD sector, consisting of the measured Lamb shift in muonic deuterium; and a λ_e sector, consisting of the Compton wavelength of the electron.

Comment. The demonstration of Table 1, which includes omitting μH and a_μ data, illustrates how decisions influence outcomes. As another example, the illustrations do not include electron or deuteron scattering, primarily because it is interesting to explore fits without it.

The Constant Finder website itself certainly allows scattering data to be incorporated. However the experimental and theoretical uncertainties from μH and μD spectroscopy are so much smaller that electron scattering adds little weight in a simple χ^2 fit. Moreover, the charge radius is not directly measured in scattering experiments, but deduced by extrapolating observations to zero momentum transfer. The radius values determined by such fits are profoundly sensitive to procedure. Reference [17], for example, found fitted proton radius values between 0.84 and 0.89 fm using a common dataset but varying the fit procedure. (The interval between 0.84 and 0.89 fm, not coincidentally, spans the entire region over which the proton's size is controversial.) Similar arguments can be made with respect to the reliability of deuteron radius values determined from eD scattering data. We have not seen similar criticisms of the μH or μD data. Section 4.6 has more discussion.

Our decision may appear unconventional, because it is commonly believed that electron scattering data is necessary and decisive. That notion appears to come from procedures choosing to *exclude* the muon data. The rationale of C10 was that R_∞, using μH data, differed from previous determinations using electron scattering by several standard deviations. That can be understood in advance, because it is a direct consequence of the strong correlation between R_∞ and r_p (Section 4.5). The additional reason C10 cited for excluding the muon data was a change in α by 3.4σ from its previous value. Yet α has changed by much larger amounts repeatedly (Figure 2). Our example uses our judgment accepting scattering experiments at face value, while by no means excluding the experiments from the game. Upcoming experiments at Mainz[18] and JLAB[19] will contribute new information. The MUSE experiment[20] will study muon-proton scattering to probe possible muon-specific interactions.

3.2.1. Validation and Caveats

Table 2 shows a sample of experimental data available on the Constant Finder site. By default 8 eH and 8 eD transitions of high precision appear. These transitions have been selected for not being overly sensitive to theoretical uncertainties. Clicking checkboxes allows adding up to 8 more transitions that involve the $1S$ state. Those states are included in C14, for instance. While the $1S2S$ transition is famous for its experimental precision, the theoretical uncertainty of the $1S$ is perhaps a thousand times larger. Because of that any use of the $1S2S$ is highly sensitive to the procedure where theory uncertainties are chosen and incorporated.[4] More information appears in Section 4.5. Where possible, the Constant Finder defaults seek to minimize sensitivity to procedural decisions.

The QED theory of electronic hydrogen and deuterium spectroscopy consists of many dozens of formulas, subsidiary formulas, and numerical parameters. It is not perfectly systematic, but includes some very tiny effects alongside much larger contributions, where not all calculations are complete. The computational core of the spectroscopic component translates the literature into about 30,000 characters of Mathematica implemented independently by each author

[4]Comparisons were done both *including* and *excluding* the $1S2S$ transition data from the fits, which with even the most optimistic theory uncertainty estimates in the literature does not have an overwhelming effect one way or the other.

on two different machines. An equivalent C++ code is estimated to need about 270,000 characters. Checking line-by-line is impossible with independent execution, so validation was done by fitting data and checking and comparing output numbers, as well as published ones, up to rounding errors.

One of our first tasks reproduced[5] the 14 values of 2-point fits shown in Figure 12. Subsequent comparisons reproduced to 13-digit accuracy and better the independent theoretical implementation of level frequencies contributing to transitions listed in Table 4 of A. Kramida's review[22], obtained from Jentschura *et al* [23]). Note that it is more demanding to compute level frequencies than transitions because many corrections cancel in transitions. The mean difference of the predictions was 65 Hz with a standard deviation of 568 Hz. We also quantify the difference of theory calculations with the ratio $\Delta f_{tt} = (f^{theory-1} - f^{theory-2})/\sigma_{exp}$ computed for each energy level. Comparisons use σ_{exp} (not estimated theory uncertainties) to avoid theoretical prejudice, and also because the comparison with the experimental uncertainty is what matters in the end. We found $\Delta f_{tt}^2 < 0.04$ in every case, with a mean for the set of 0.003 and standard deviation of 0.010. With few exceptions, the C10-selected transitions are simply those with the smallest experimental uncertainties. These transitions are listed with numerous correlation parameters[6] and additive corrections discussed in the Appendix. To eliminate a possibility those data are special, we fit the rest of the levels listed in Table 4 of Ref. [22] and checked its statements.[7]

3.3. A Global Fit to Standard Model Physics

Table 4 shows the Constant Finder results fitting the fundamental constants shown. This illustration minimizes a basic χ^2 statistic given by Eq. 4 and neglecting theory uncertainties. Before we discuss the results in depth, a high-level picture is useful. Figure 6 is a simple schematic showing the relationships between the fit elements of the illustration. A line between a fit parameter and a

[5]We thank Th. Udem for patient explanation of the errors of the 2-point fit procedure used in Ref. [21] and providing computer code to check it.

[6]Including the input correlations listed in C10 for the *experimental* data had negligible effects on our QED-EW study: r_p was the same within our uncertainty. Indeed the $1S2S$ datum is listed as completely *uncorrelated*

[7]Kramida[22] discusses 10 cases of calculations differing from experiment by more than 2σ, which all involve $n = 3$ or $n = 6$ levels. They have a nearly constant energy shift attributed to systematic experimental error. We verified those discrepancies exist as described.

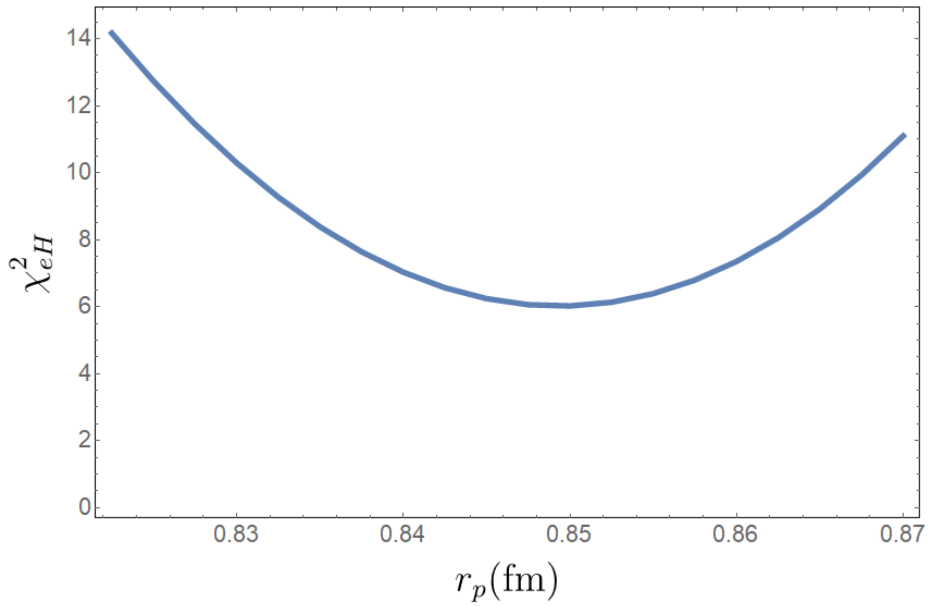

Figure 5. χ^2_{eH} versus r_p, with R_∞, α, and r_d fixed at the fitted values of Line 1 of Table 4. When the muonic data is included in the analysis, the electronic hydrogen spectroscopy data favors a 'small' proton radius value $\sim .85$ fm.

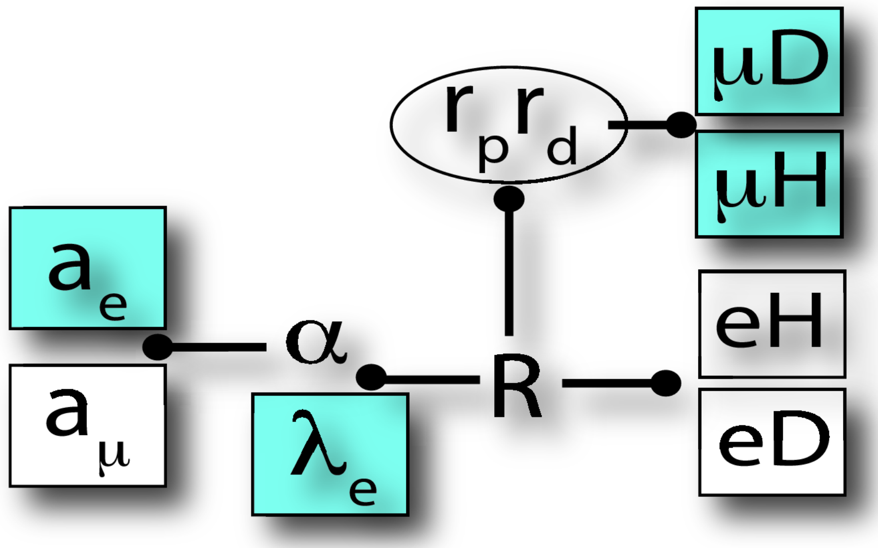

Figure 6. Schematic of the global fit assuming Standard Model physics. A line between a fit parameter and a data sector indicates a dependency. Strong dependencies are indicated by blue data sectors. For instance, a_e (blue) dominates the fit to α, while a_μ, which depends directly on α, does not. The Rydberg is strongly dependent on μH and μD data because the experimental and theoretical uncertainties of that data are very small.

Table 3. Experimental data compared to calculations by the Constant Finder. Calculated values are based on a Standard Model fit to Table 2 data. Fitted constants for the fit appear in Line 1, Table 4.

Experimental datum	Experimental value	Fitted value	σ_{expt}
$\nu_H(2S1/2 - 8S1/2)$ [Hz]	$7.70649350012000 \times 10^{14}$	$7.70649350015089 \times 10^{14}$	8600.
$\nu_H(2S1/2 - 8D3/2)$ [Hz]	$7.70649504450000 \times 10^{14}$	$7.70649504448244 \times 10^{14}$	8300.
$\nu_H(2S1/2 - 8D5/2)$ [Hz]	$7.70649561584200 \times 10^{14}$	$7.70649561577394 \times 10^{14}$	6400.
$\nu_H(2S1/2 - 12D3/2)$ [Hz]	$7.99191710472700 \times 10^{14}$	$7.99191710480623 \times 10^{14}$	9400.
$\nu_H(2S1/2 - 12D5/2)$ [Hz]	$7.99191727403700 \times 10^{14}$	$7.99191727407767 \times 10^{14}$	7000.
$\nu_H(2P1/2 - 2S1/2)$ [Hz]	$1.05784500000000 \times 10^{9}$	$1.05783220761556 \times 10^{9}$	9000.
$\nu_H(2S1/2 - 2P3/2)$ [Hz]	9911200000	9911209318	12000.
$\nu_H(2P1/2 - 2S1/2)$ [Hz]	1057862000	1057832208	20000.
$\nu_D(2S1/2 - 8S1/2)$ [Hz]	$7.708590412457 \times 10^{14}$	$7.7085904124256 \times 10^{14}$	6900.
$\nu_D(2S1/2 - 8D3/2)$ [Hz]	$7.708591957018 \times 10^{14}$	$7.70859195700519 \times 10^{14}$	6300.
$\nu_D(2S1/2 - 8D5/2)$ [Hz]	$7.708592528495 \times 10^{14}$	$7.70859252845263 \times 10^{14}$	5900.
$\nu_D(2S1/2 - 12D3/2)$ [Hz]	$7.99409168038 \times 10^{14}$	$7.99409168041396 \times 10^{14}$	8600.
$\nu_D(2S1/2 - 12D5/2)$ [Hz]	$7.994091849668 \times 10^{14}$	$7.9940918497316 \times 10^{14}$	6800.
$\nu_D(2P1/2 - 2S1/2)$ [Hz]	1059280000	1059220261	60000
$\nu_D(2S1/2 - 2P3/2)$ [Hz]	9912610000	9912815235	300000
$\nu_D(2P1/2 - 2S1/2)$ [Hz]	1059280000	1059220261	60000
a_e	0.00115965218072	0.00115965218078	2.8×10^{-13}
a_μ	0.00116592089	0.00116591840	6.3×10^{-10}
$\Delta E_{LS}(\mu H)$ [meV]	202.3706	202.3705	0.0023
$\Delta E_{LS}(\mu D)$ [meV]	202.8785	202.8785	0.0034
λ_e [m]$/10^{-12}$	2.4263102367	2.4263102356	1.1×10^{-9}

data sector indicates a dependency. Strong dependencies have blue data sectors: the μH (μD) sector dominates the fit to r_p (r_d) via R_∞. The electron's anomalous moment dominates the fit to α; and the electron's Compton wavelength λ_e dominates the fit to R_∞.

For the fit omitting μH (Line 3 of Table 4), R_∞ and r_p have a strong positive correlation[8] (0.59). For the fit omitting μD (Line 4), R_∞ and r_d have a strong positive correlation (0.75). For the fits omitting μH and μD (Lines 5 and 9), R_∞, r_p, and r_d are all strongly positively correlated with one another, with correlations exceeding 0.82. See Table 5. Since it is possible to fit R_∞, r_p, and

[8]The correlation of R_∞ and r_p exceeds 0.995 when the $1S2S$ level is included with no theoretical uncertainties. That is an example of exquisite sensitivity to procedural decisions. Theoretical uncertainties of order one thousand times the experimental ones nullify the effect of the transition.

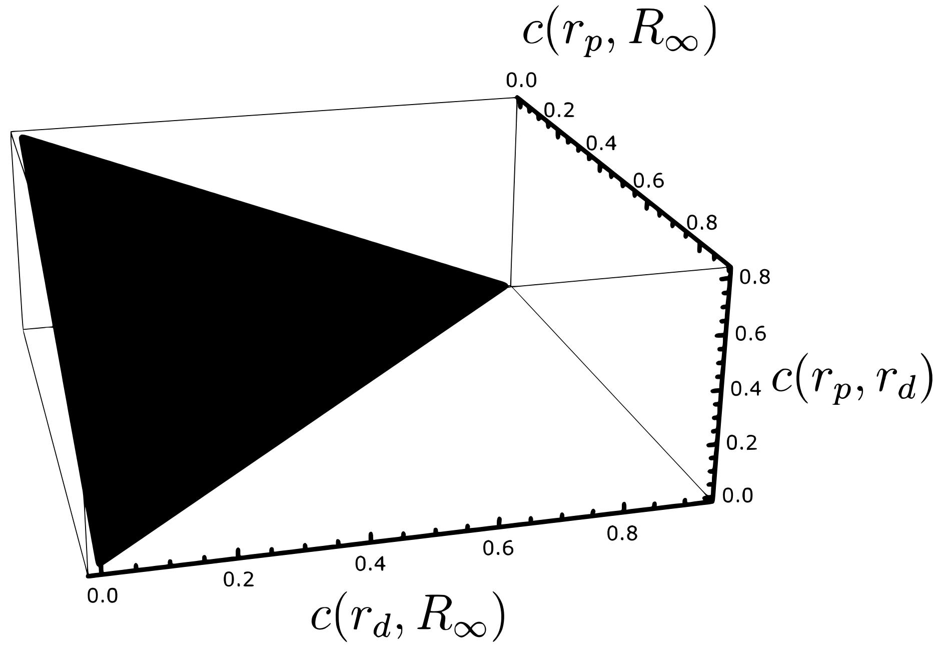

Figure 7. The non-trivial correlations of Line 5, Table 4, between $r_p - R_\infty$, $r_d - R_\infty$, and $r_p - r_d$. Non-trivial correlations emerge only after removing the μH, μD data from the fit, and are discussed in the text.

Table 4. Fitted values of $\delta R_\infty/R^*_\infty$, $\delta\alpha/\alpha^*$, r_p, r_d for global fits with different observables omitted, where R^*_∞, α^* are reference values. Standard Model physics is assumed. Line 9 omits all muonic observables and gives fitted values consistent with the values of C14. There is a 2.1σ discrepancy between the r_p values of Line 1 and Line 9. The first line, *omit none*, generates Table 3.

line	omit	$(\delta R_\infty/R^*_\infty)/10^{-12}$	$(\delta\alpha/\alpha^*)/10^{-10}$	r_p fm	r_d fm
1	$none$	$-13.4(2.9)$	$-2.2(2.2)$	$0.84088(26)$	$2.12870(13)$
2	λ_c	$-13.4(2.9)$	$-2.7(2.4)$	$0.84088(26)$	$2.12870(13)$
3	μH	$-10.1(3.6)$	$-2.2(2.2)$	$0.859(11)$	$2.12870(13)$
4	μD	$-14.7(4.4)$	$-2.2(2.2)$	$0.84088(26)$	$2.1265(55)$
5	μH, μD	$3.4(9.5)$	$-2.2(2.2)$	$0.883(19)$	$2.1433(96)$
6	a_e	$-13.4(2.9)$	$-0.068(5.)$	$0.84088(26)$	$2.12870(13)$
7	a_μ	$-13.4(2.9)$	$-2.2(2.2)$	$0.84088(26)$	$2.12870(13)$
8	a_e, a_μ	$-13.4(2.9)$	$-0.086(5.)$	$0.84088(26)$	$2.12870(13)$
9	μH, μD, a_μ	$3.4(9.5)$	$-2.2(2.2)$	$0.883(19)$	$2.1433(96)$
10	eH	$-12.0(3.9)$	$-2.2(2.2)$	$0.84087(26)$	$2.12870(13)$
11	eD	$-15.2(4.4)$	$-2.2(2.2)$	$0.84088(26)$	$2.12870(13)$
12	eH, eD	$-500(1100)$	$-2.7(2.2)$	$0.84087(26)$	$2.12870(13)$
13	eD, μD	$-15.2(4.4)$	$-2.2(2.2)$	$0.84088(26)$	–

r_d, with all other constants such as α held fixed, that has generally been done in published tables. The rationale is that R_∞ does not by itself improve the fitting of α. However when there are discrepancies afoot, and controversies about (say) μH charge radius determinations, one cannot rely on a method partitioning data too narrowly. When μH or μD data is included the large correlations go away, and no correlations exceed 0.04.

The correlations of Table 5 are shown graphically in Fig. 7. The correlations can be understood as follows. μH dominates the fit to r_p but has no R_∞ dependence. When it is removed from the fit, the eH and eD data, along with λ_e, determine R_∞ while r_p, the only free parameter remaining in the eH sector (see Fig. 6), floats to a best-fit value on the basis of the fitted value of R_∞. r_d is determined almost entirely by μD. By similar reasoning, r_d and R_∞ are correlated when μD is removed. Finally, when μH and μD are removed, the correlation between r_p and r_d occurs through the fitted value of R_∞.

Table 5. The correlation matrix of the fit of Line 9, Table 4 omitting all muon data.

$$\begin{array}{cccc} R_\infty & \alpha & r_p & r_d \end{array}$$
$$\begin{bmatrix} 1.00 & 0.00356 & 0.888 & 0.927 \\ 0.00356 & 1.00 & 0.00382 & 0.00395 \\ 0.888 & 0.00382 & 1.00 & 0.822 \\ 0.927 & 0.00395 & 0.822 & 1.00 \end{bmatrix}$$

We now examine Table 4 more closely. The table shows the (in some cases, extreme) dependence of fitted values of the fundamental constants on the choice of input data. Line 9 of Table 4 omits all muonic data from the fit, as done in the final adjustments of C10 and C14[9]. As consistent, the fitted values of R_∞, α, r_p, and r_d of Line 9 are all within 1σ of the values recommended by C14, which we adopt as our reference values[10].

In contrast Line 1 of Table 4 shows the global fit to all Table 3 data, including the muonic data. The fit finds a Rydberg value R_∞ more than 4σ from the value recommended by C14. It is often reported that QED has been tested severely by the "most precise physical constant", but the variations of procedure, *all presenting a good fit*, shows the Rydberg can indeed move.

The fit also finds a proton radius value $r_p = 0.84088(26)$ fm, which differs from the radius value of Line 9 by 2.1σ and from the C14 recommended value by 5.6σ. Chi-squared contours for the Line 1 and Line 9 fits are shown in Figs. 8 and 9, respectively. The Line 9 fit shows a soft degeneracy between R_∞ and r_p and between R_∞ and r_d, which is discussed in Sec. 4.5.

[9]The muonic deuterium data were not available prior to the C10 adjustment. The C14 adjustment has not been released.

[10]Our reference values are as follows: $R_\infty^* = 10973731.568508(65)\,\mathrm{m}^{-1}$; $\alpha^* = 7.2973525664(17) \times 10^{-3}$; $r_p = 0.8751(61)$ fm; and $r_d = 2.1413(25)$ fm

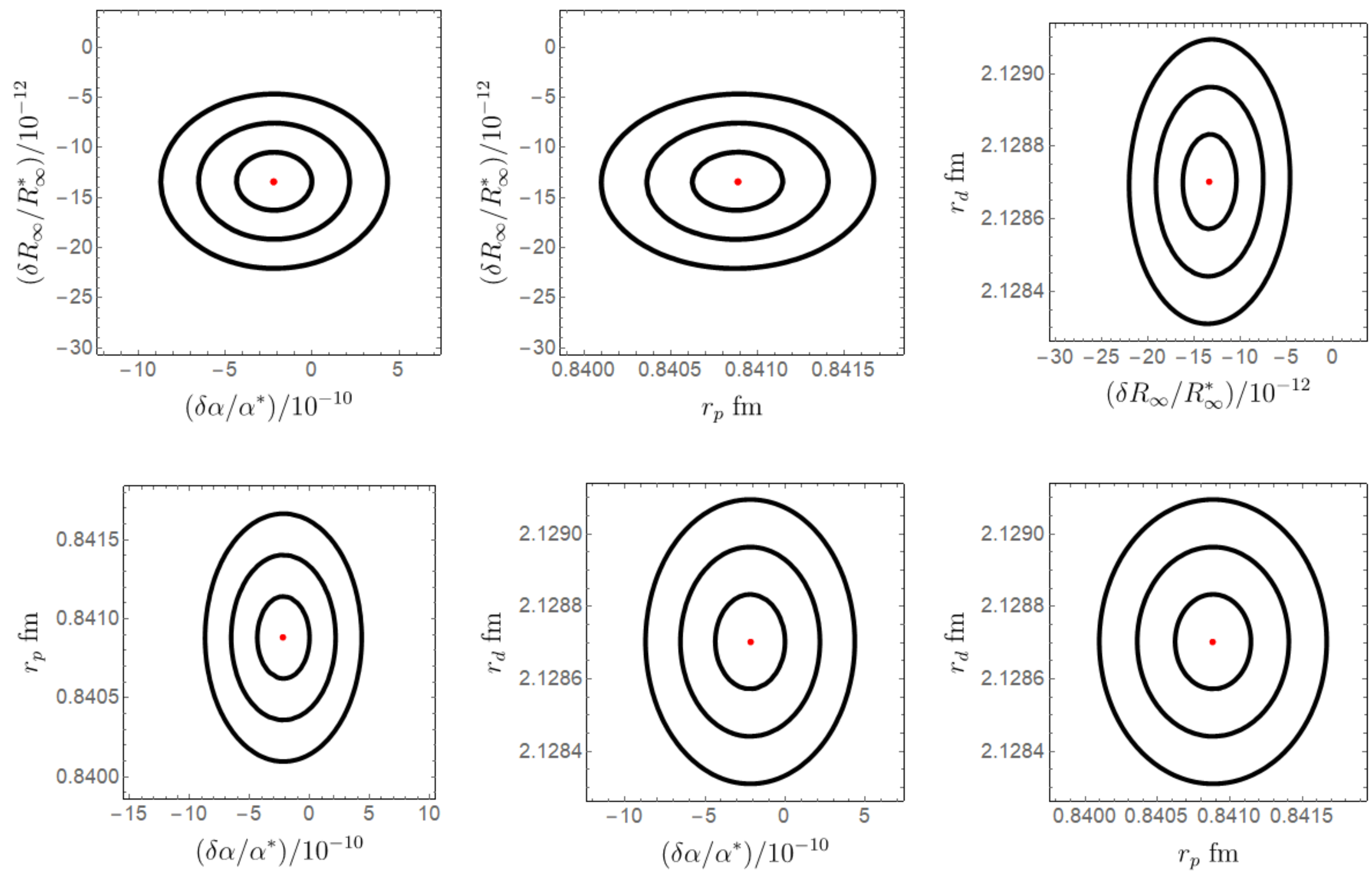

Figure 8. 1, 2, and 3σ chi-squared contours for the full global fit in fit-parameter space. In each subplot the fit parameters not shown are fixed at the best fit values of Line 1, Table 4.

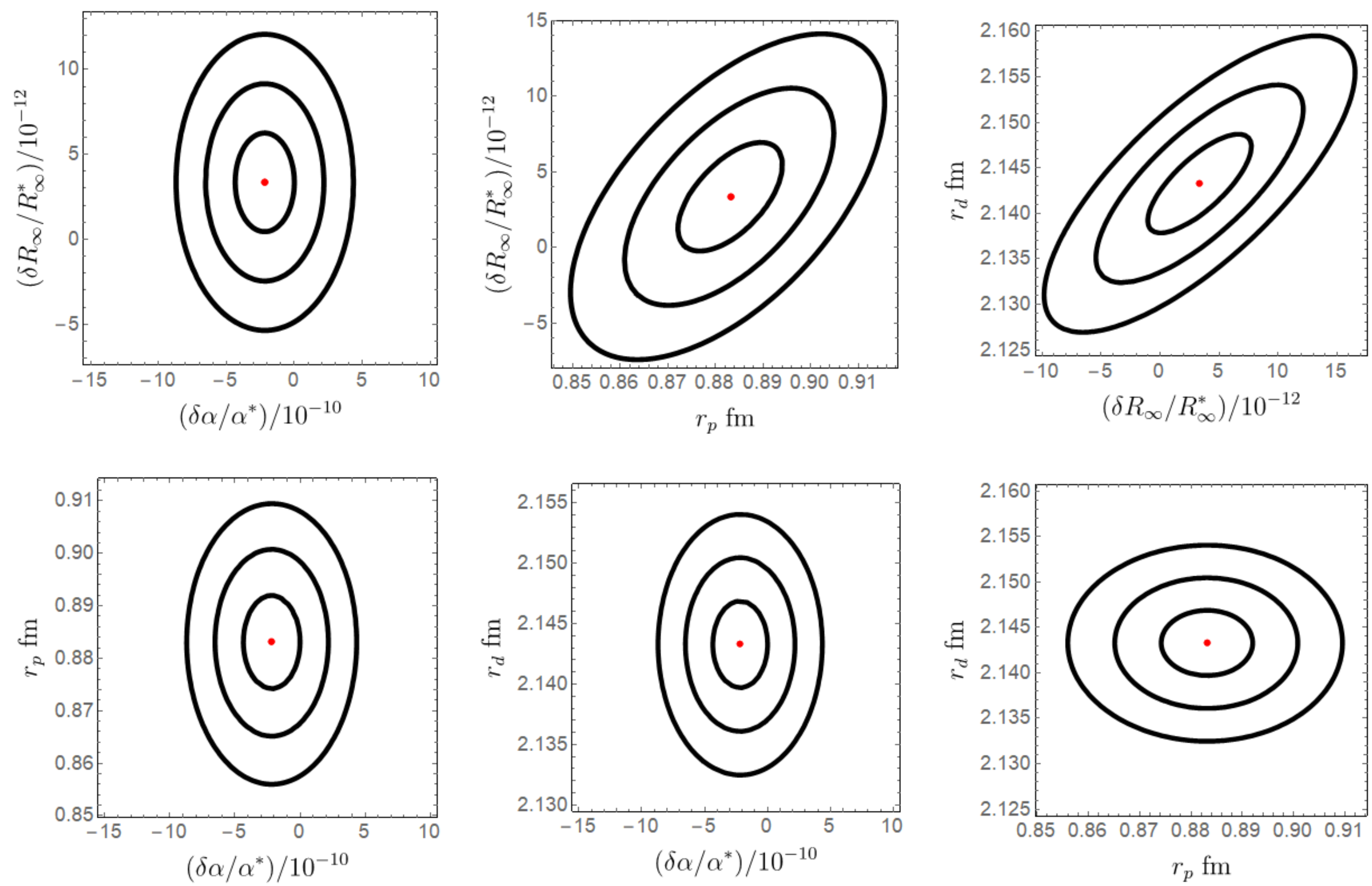

Figure 9. 1, 2, and 3σ chi-squared contours for the global fit omitting all muonic data in fit-parameter space. In each subplot the fit parameters not shown are fixed at the best fit values of Line 9, Table 4. An approximate degeneracy between R_∞ and r_p and R_∞ and r_d can be seen in the top middle and top right subplots, respectively. The degeneracy is discussed in Fig. 6.

The discrepancy between the proton radius values of Lines 1 and 9 is due to the precision of the muonic hydrogen datum. The eH spectroscopy data *with no reference to electron scattering* favors $r_p \sim .872(10)$ fm; see Line 9 of Table 4 as well as Section 4.6 and Fig. 13. However the μH datum, which favors $r_p \sim 0.84$ fm, dominates the fit, pulling the fitted proton radius value to its value.

The fitted correlation matrix shown in Table 5 explains this quantitatively. In the fit of Line 5, Table 4 (*excluding* all muonic data) the values of R_∞, r_p and r_d are mutually correlated at order "1." More discussion appears in the caption of Table 7. Since it is possible to fit these parameters with all other constants such as α held fixed, that has generally been done in published tables. The rationale is that R_∞ does not by itself improve the fitting of α. However when there are discrepancies afoot, and controversies about (say) μH charge radius determinations, one cannot rely on a method partitioning data too narrowly.

Figure 10 rather clearly shows the effect of *including* μH data. The figure is made adjusting the experimental uncertainty $\sigma(\mu H)$ as a free parameter, while otherwise defined by Line 3 of Table 4. As $\sigma_{\mu H}$ is increased, the fitted r_p approaches the value from eH. Increasing $\sigma_{\mu H}$ by a factor above 200 (!) dilutes its information enough to be the same as omitting it.

For simplicity the muonic deuterium (μD) datum has been omitted in making Figure 10. When included, the μD datum dominates the fit to r_d exactly parallel to the above. When the Rydberg is fit by generic least squares using eH, eD, μH, μD the muonic data is decisive, unless decisions are made to render it otherwise.

Inspecting Table 6, we find χ^2 in each sector is well-controlled for all fits, with the (jarring) exception of the a_μ sector. The a_μ sector, when it is included in the global fit, contributes 15.7 units of chi-squared despite containing only one experimental datum, the experimental value of the muon anomalous moment measured at BNL. Hence we find $|a_\mu^{exp} - a_\mu^{th}| = \sqrt{15.7}\sigma = 3.9\sigma$, where the superscripts exp and th denote experimental and theoretical values. 3.9σ is the same magnitude as the discrepancy reported in Ref. [5]. This is not quite a coincidence: With α fixed, one finds it trivially. But one needs an objective reason for α to be fixed.[11]

Tables 4 and 6 suggest the existence of *one* muon experimental anomaly, but they did not need to. While the analysis is very detailed compared to piecemeal

[11] It is easy to fix α using a_e. The wisdom of putting immense weight on a single experiment and one rendition of theory is another issue.

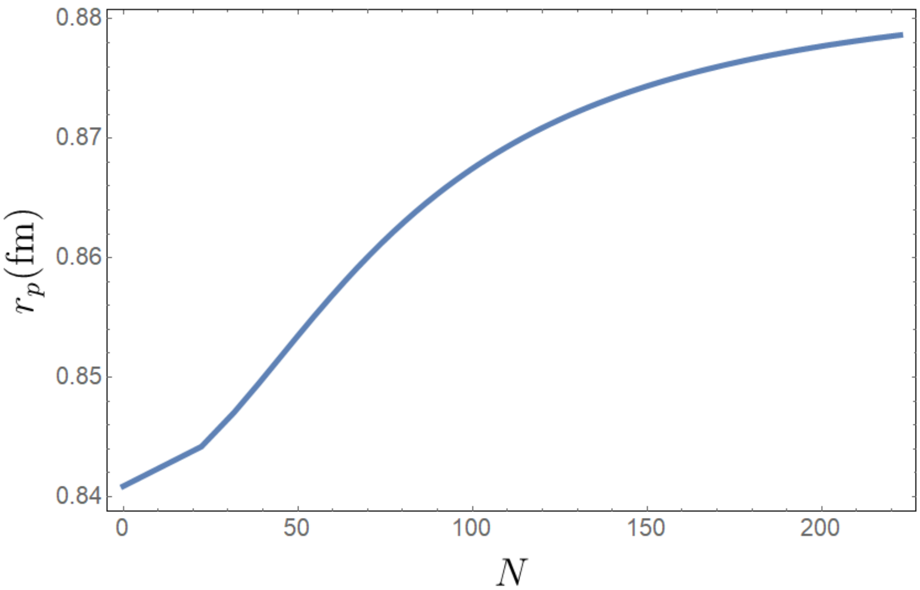

Figure 10. The change in the fitted value of r_p from adjusting the experimental error of the μH datum $\Delta E_{LS}(\mu H) \rightarrow N\sigma$, where σ is the experimental uncertainty. As N is increased r_p moves from $.84$ fm, the value favored by the μH datum, to $.88$ fm, the value favored by the eH sector. The global fit here is the same as Line 1, Table 4 omitting muonic deuterium.

Table 6. Contributions to χ^2 for global fits with different observables omitted. dof stands for the number of degrees of freedom. Standard Model physics is assumed. The a_μ sector, when it appears in the global fits, contains only one experimental observable while contributing 15.7 units of chi-squared. All other sectors across all fits have well-controlled contributions to χ^2.

line	omit	χ^2	dof	$\chi^2_{\lambda_c}$	$\chi^2_{\mu H}$	$\chi^2_{\mu D}$	$\chi^2_{a_e}$	$\chi^2_{a_\mu}$	χ^2_{eH}	χ^2_{eD}
1	$none$	27.5	17	0.18	0.0012	0.000095	0.042	15.7	7.4	4.3
2	λ_c	27.3	16	–	0.0012	0.000095	0	15.7	7.3	4.2
3	μH	25.1	16	0.18	–	0.00043	0.043	15.7	4.8	4.4
4	μD	27.3	16	0.18	0.00076	–	0.042	15.7	7.2	4.2
5	$\mu H, \mu D$	22.8	15	0.19	–	–	0.045	15.7	3.3	3.5
6	a_e	27.3	16	0.000013	0.0012	0.000094	–	15.7	7.3	4.3
7	a_μ	11.8	16	0.18	0.0012	0.000095	0.042	–	7.3	4.3
8	a_e, a_μ	11.6	15	0	0.0012	0.000094	–	–	7.3	4.3
9	$\mu H, \mu D, a_\mu$	7.1	14	0.19	–	–	0.044	–	3.3	3.5
10	eH	20.0	9	0.18	0	0	0.042	15.7	–	4.1
11	eD	23.1	9	0.18	0.00062	0	0.042	15.7	7.2	–
12	eH, eD	15.7	1	0	0	0	0	15.7	–	–
13	$eD, \mu D$	23.1	8	0.18	0.00062	–	0.042	15.7	7.2	–

comparisons, we think it is not thorough enough. What is better judgment: To completely banish a_μ or find a way the data might make sense? What are the effects of doubling all the experimental uncertainties, and adding hefty theory uncertainties either to all or selected data? The reader is invited to explore. We also find this interesting: Contrary to some claims, we can find no evidence for *two* muon anomalies, with the second involving the data for μH and μD. In fact, varying r_p inside the eH sector of χ^2 while keeping α, R_∞, and r_d fixed at the fitted values of Line 1 of Table 4 finds the favored value for r_p in the eH sector $\sim .85(01)$ fm, consistent with the favored radius value of the μH datum: see Fig. 5.

3.4. A Global Fit to an Alternative

The global fits to the Standard Model of Sec. 3.3 reveal a poor fit when a_μ is included. We turn to alternatives. Depending on one's particular bent, one might seek to explain the discrepancy within the Standard Model, by adjusting fit assumptions (theory uncertainties and so forth), or beyond the Standard Model, by introducing new physics into the fit. While not all alternatives need to seek new physics, we will provide an example, to illustrate that portion of the Constant Finder site's capabilities.

As discussed in Sec. 2.1.1, let X denote a massive boson that interacts with the leptons of the Standard Model via a simple interaction, with Lagrangian: $\mathcal{L} \supset \lambda X \bar{\psi}\psi$ or $\lambda X_\mu \bar{\psi}\gamma_\mu\psi$, in the case X is a vector. Then X will contribute to a_e and a_μ, with its respective contributions mediated by the two new parameters m_X and λ_X, or $\alpha_X = \lambda_X/4\pi$. For a lepton mass m_ℓ it is well known that contributions to the anomaly will scale like m_ℓ^2/m_X^2 when $m_X >> m_\ell$. This makes the muon anomaly generally more sensitive to the new contributions in the range $m_e << m_X \lesssim m_\mu$.

Particle-X can also be coupled to protons and neutrons, affecting atomic and muonic spectra. For simplicity the coupling to neutrons will be set to zero. Nothing determines the signs of couplings, which we leave undetermined in searching over different fits. The signs of couplings cancel out in a one-loop anomalous moment, but do not cancel in Yukawa-type interactions between protons and electrons, say.

The exercise of adding two parameters to the global fit is a completely neutral investigation. If the global fit improves with the two new parameters it can be considered statistically significant, and potentially interesting. Meanwhile, there may be many subtle reasons for the improvement, completely unrelated to any new physics. The physical consistency of any particular model will generally hinge on an entire universe of specific predictions and constraints outside the scope of this paper. Our attention here is restricted to illustrating the fitting process.

For reasons that will become clear we fix the mass $m_X = 50$ MeV and represent $\alpha_X = \xi m_X^2$. We then re-determine R_∞, α, r_p, r_d and ξ from best-fit values.

Tables 7 and 8 are the same as Tables 4 and 6 but with an additional parameter ξ added to the fits. The fourth column of Table 7 shows $\Delta\chi^2$, which is the improvement in chi-squared compared to the corresponding fit to the Standard Model (Table 6). $\Delta\chi^2$ is ~ 15 for the fits that include the a_μ datum, due to improvements in the fits to the a_μ sector, with $\chi^2_{a_\mu} << 1$ across all relevant fits.

Table 7. Contributions to χ^2 for global fits with different observables omitted. A no-name boson (Section 2.1.1) with mass $m_\chi = 50MeV$ and coupling α_X has been introduced. The a_μ sector now has well-controlled χ^2 across all fits. $\Delta\chi^2$ gives the improvement in χ^2 due to the model variation over the corresponding Standard Model fit of Table 6. $R_B = \sqrt{\chi^2/dof}$ is the Birge ratio. Overfitting is discussed in the text.

line	omit	χ^2	dof	R_B	$\Delta\chi^2$	$\chi^2_{\lambda_c}$	$\chi^2_{\mu H}$	$\chi^2_{\mu D}$	$\chi^2_{a_e}$	$\chi^2_{a_\mu}$	χ^2_{eH}	χ^2_{eD}
1	$none$	12.5	15	.91(10)	15.0	1.0	0.0011	0.000096	0.24	0.019	7.0	3.3
2	λ_c	11.2	14	.89(10)	16.1	–	0.0011	0.000096	0	0.0030	6.9	3.3
3	μH	10.2	14	.85(10)	14.9	1.0	–	0.00038	0.24	0.026	4.7	3.4
4	μD	12.3	14	.94(10)	15.0	1.0	0.00068	–	0.24	0.019	6.8	3.2
5	$\mu H, \mu D$	8.2	13	.79(11)	14.6	1.0	–	–	0.24	0.037	3.3	3.0
6	a_e	11.2	14	.89(10)	16.1	0	0.0011	0.000095	–	0.0030	6.9	3.3
7	a_μ	11.8	14	.92(10)	0.017	0.093	0.0012	0.000095	0.022	–	7.4	3.3
8	a_e, a_μ	7.0	13	.73(11)	4.6	0	0.000053	0.000088	–	–	3.5	3.0
9	$\mu H, \mu D, a_\mu$	6.9	13	.73(11)	0.23	0	–	–	0	–	3.3	3.0
10	eH	5.4	7	.88(17)	14.7	1.0	0	0	0.24	0.035	–	3.2
11	eD	8.1	7	1.08(17)	15.0	1.0	0.00056	0	0.24	0.020	6.8	–
12	eH, eD	0	0	–	15.7	0	0	0	0	0	–	–
13	$eD, \mu D$	8.1	6	1.16(18)	15.0	1.0	0.00069	–	0.24	0.020	6.8	–

Table 8. Fitted values of R_∞, α, r_p, r_d for global fits with different observables omitted. A no-name boson (Section 2.1.1) with mass $m_\chi = 50MeV$ and coupling $\alpha_X = \xi m_X^2$ has been introduced.

line	omit	$(\delta R_\infty/R^*_\infty)/10^{-12}$	$(\delta\alpha/\alpha^*)/10^{-10}$	r_p fm	r_d fm	ξ MeV$^{-2}/10^{-11}$
1	*none*	$-12.5(2.9)$	$-5.1(2.3)$	0.84115(27)	2.12879(13)	1.52(39)
2	λ_c	$-12.4(2.9)$	$-6.5(2.6)$	0.84117(27)	2.12879(13)	1.59(40)
3	μH	$-9.4(3.6)$	$-5.1(2.3)$	0.858(11)	2.12879(13)	1.51(39)
4	μD	$-14.1(4.4)$	$-5.1(2.3)$	0.84115(27)	2.1261(055)	1.52(39)
5	$\mu H, \mu D$	2.4(9.6)	$-5.1(2.3)$	0.879(19)	2.1415(96)	1.50(39)
6	a_e	$-12.5(2.9)$	$-0.1(5.0)$	0.84117(27)	2.12879(13)	1.59(40)
7	a_μ	$-13.6(3.2)$	$-1.5(4.9)$	0.84082(49)	2.12868(19)	$-0.3(2.3)$
8	a_e, a_μ	4.0(9.0)	0.0(5.0)	0.8463(26)	2.13054(90)	30(15)
9	$\mu H, \mu D, a_\mu$	2.5(9.6)	0.0(5.0)	0.883(20)	2.1428(97)	$-1.1(2.3)$
10	eH	$-11.1(3.9)$	$-5.1(2.3)$	0.84114(27)	2.12879(13)	1.50(39)
11	eD	$-14.3(4.4)$	$-5.1(2.3)$	0.84115(27)	2.12879(13)	1.52(39)
12	eH, eD	$-1300(1100)$	$-6.5(2.6)$	0.84115(27)	2.12879(13)	1.57(40)
13	$eD, \mu D$	$-14.3(4.4)$	$-5.1(2.3)$	0.84115(27)	–	1.51(40)

Each fit in Table 8 represents a candidate solution[12] to the muon experimental anomalies, valid in its own domain. For instance, Line 1 of Table 8, fitting all Table 2 data, solves the proton size puzzle in favor of the smaller muonic radius ~ 0.84 fm. The mechanism is somewhat intricate. The muonic anomaly is quite sensitive to the mass range $m_X \sim 50$ MeV. For the same mass range the eH Lamb shift and a_e approximately depend on $\xi = \alpha_X/m_X^2$. The extra attraction caused by X between electron and proton decreases r_p in eH to be compatible with μH. The fine structure constant moves because α and α_X/m_X^2 compete to fit the data for a_e, provided m_X is not too small. The fit of Line 1 also shifts R_∞ by 4σ relative to the C14 value, while the fit shows this is tolerable.

For another example Line 9, omitting all muonic data, reverts as expected to favor the larger electronic radius ~ 0.88 fm. Line 9 then finds only a nominal shift in R_∞ relative to C14.

The Birge ratios of Table 7 are close to one within uncertainties, with a few exceptions. Lines 3 and 5, omitting μH and μH, μD, have $R_B = .85(10)$ and $R_B = .79(11)$. However in both cases Model-X is needed to reduce χ^2 in the

[12] A tentative solution, up to further experimental constraints and tests

a_μ sector (see Lines 3 and 5 of Table 4). Line 8, omitting the muon and electron anomalous moments, has $R_B = .73(11)$. The corresponding line of Table 4, which assumes Standard Model physics, shows reasonable fits in all sectors. By its accounting, Model-X is not needed in the fit. Finally, Line 9 of Table 7, omitting all muonic data, has $R_B = .73(11)$. Omitting all muonic data from the fit removes the muon experimental anomalies from the problem, along with the need for Model-X or any new physics.[13]

Including Model-X in the global fits does not significantly alter the Standard Model correlations between R_∞, α, r_p, and r_d, discussed in Fig. 6. In addition, the correlation of ξ with the Standard Model fit parameters is negligible (< 0.01 across all fits).

Table 9. Fitted values of $\delta R_\infty/R^*_\infty$, $\delta\alpha/\alpha^*$, r_p, r_d, and $\xi = \alpha\chi/m_\chi^2$ for the full global fit with m_χ fixed at different values. R^*_∞, α^* are reference values. Line 3 of this table corresponds to Line 1 of Table 8.

m_χ MeV	$\Delta\chi^2$	$(\delta R_\infty/R^*_\infty)/10^{-12}$	$(\delta\alpha/\alpha^*)/10^{-10}$	r_p fm	r_d fm	ξ MeV$^{-2}/10^{-11}$
15	6.6	−10.9(3.1)	−10.6(3.9)	0.84157(37)	2.12894(16)	4.3(1.7)
25	12.4	−11.4(3.0)	−8.9(2.9)	0.84147(31)	2.12890(14)	3.45(98)
50	15.0	−12.5(2.9)	−5.1(2.3)	0.84115(27)	2.12879(13)	1.52(39)
100	15.5	−13.0(2.9)	−3.6(2.2)	0.84101(26)	2.12875(13)	0.70(18)
150	15.6	−13.1(2.9)	−3.1(2.2)	0.84097(26)	2.12873(13)	0.49(12)
200	15.6	−13.1(2.9)	−3.0(2.2)	0.84096(26)	2.12873(13)	0.40(10)
300	15.6	−13.2(2.9)	−2.8(2.2)	0.84094(26)	2.12872(13)	0.320(81)

Table 9 shows the results of global fits to all Table 2 data for different values of m_X. The second column shows the improvement in chi-squared compared to the corresponding fit to the Standard Model (Line 1 of Table 6). $\Delta\chi^2$ is 6.6 for $m_X = 15$ MeV, increasing to ~ 15 for $m_X > 50$ MeV, where it remains for masses m_X out past a GeV. The fits favor a proton radius $r_p \sim 0.84$ fm. Global fits with mass $m_X \gtrsim 30$ MeV find $\chi^2_{a_\mu} < 4$ (corresponding to $|a_\mu^{expt} - a_\mu^{th}| < 2\sigma$), with χ^2 in all other sectors well-controlled. The entire region of $m_X \gtrsim 30$ MeV provides an alternative to excluding a_μ from consideration.

Figure 11 shows the region, in red, in the (m_X, α_X) plane favored by the Table 9 analysis. The red band represents the fitted value of α_X for given mass

[13]Birge ratios are not shown in Table 4 because the fits assuming Standard Model physics fit only the Rydberg sector parameters, and no nuisance parameters. Hence overfitting cannot be an issue.

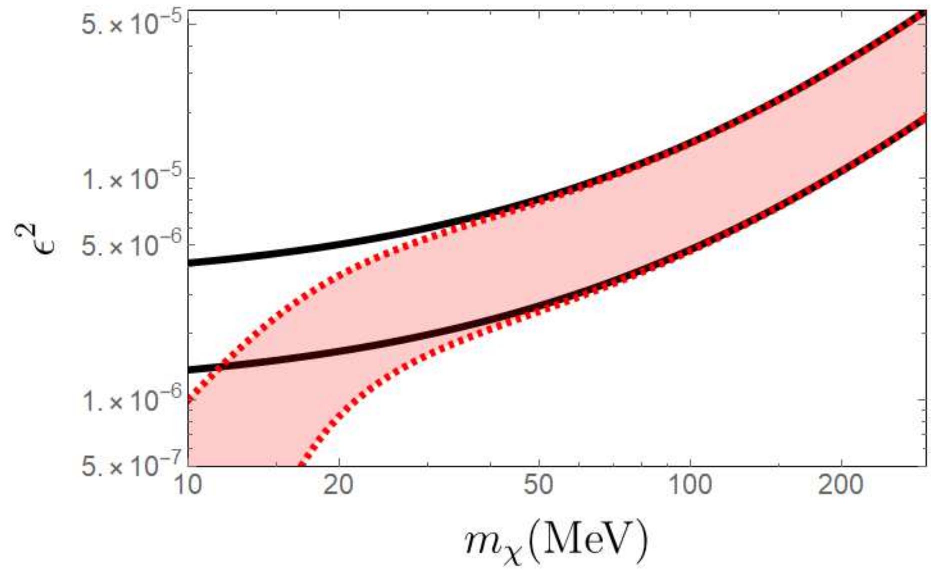

Figure 11. Region in the (m_X, α_X) plane favored by the no-name analysis (red). The red band represents the fitted value of α_X for given mass m_X, plus or minus 2σ. Within the red band the improvement $\Delta\chi^2 > 6$ for $m_X > 10MeV$, dropping rapidly to $\Delta\chi^2 > 15$ for $m_X > 50MeV$, and then decreasing monotonically at a much slower rate for larger m_X. No upper limit on m_X can be resolved, The solid black lines define a piecemeal solution region seeking only to solve the muon g-2 anomaly with α, R_∞, r_p, and r_d fixed at C14 recommended values. The region is is falsely restrictive by not implementing a self-consistent global fit.

m_X, plus or minus 2σ. It provides candidate solutions to the muon g-2 anomaly for values of $m_X \gtrsim 30$ MeV. The solid black lines define a default piecemeal solution region which fits the muon g-2 anomaly with α, R_∞, r_p, and r_d fixed at reference values. This region is identical to the green band of Fig. 22 of Ref. [24]. The candidate solution region of the red band ($m_X \gtrsim 30$ MeV) differs visibly from the default solution region for $m_X \lesssim 50$ MeV. If the global fits of Table 9 had shifted α from its reference value by a greater amount (certainly possible, if a different model were assumed), that difference would be compounded. Figure 11 represents a caution against fitting or placing limits on model parameters without refitting self-consistent fundamental constants. It is faulty in principle, and generally leads to incorrectly restrictive constraints.

Comment. There has been great interest recently in light weakly, interacting bosons known as ”dark photons”. These models assume more structure at the outset than Model-X. For example the dark photon models (as currently implemented) predict a sign for couplings contradicting the solution found here. Several experimental studies might exclude portions of Fig. 11 if the dark photon parameter ϵ^2 is transcribed to α_X. Yet the implications of most experimental studies are quite model-dependent and need additional assumptions to apply. A paper including such considerations can be found in Ref. [15]. The work reported here restricts attention to illustrating the potential power of the Constant Finder concept.

4. Conclusion

The sensitivity of the fundamental constants to procedural decisions is an open secret in high-precision QED, but the (disturbing) extent of the sensitivity is seldom appreciated. The fundamental constants are highly sensitive to the choices of data and theory inputs as well as the treatment of experimental and theoretical uncertainties. The relationships are global and there does not seem to be a universal “best” constant or a “best” way to proceed.

Each *set* of constants should be considered in relation to the assumptions and correlations that went into the set’s determination. As a corollary, testing QED and placing limits on new physics requires a global approach which appropriately accounts for assumptions and correlations. This small shift in perspective has important consequences.

For instance, separate piecemeal fits to ep scattering data and muonic hydrogen spectroscopy data (with many parameters fixed) give discrepant proton radius values. However a global fit to all Table 2 data, allowing relevant parameters to float to best-fit values, removes the discrepancy, for the price of shifting R_∞ by 4σ.

The muon g-2 anomaly is a second example of the importance of a global view. The studies done here indicate it demands new physics or a drastic revision of the uncertainties that enter the determination of a_μ. In either case, the chi-squared function will surely change, and with it the fitted values of the constants, making a global fit necessary. In the case of new physics, a global fit becomes all the more central, since new information will generally shift the favored values of the previous constants. Immense importance is sometimes given to exclusion limits, where correct experiments might be dismissed as faulty, or correct theory can be forgotten as wrong. The general trend of global fits is to weaken exclusion limits compared to the internally inconsistent practice of keeping old constants fixed.

As we have experienced, the effort required to make one's own global fits from scratch is quite significant. Now that the work has been done the Constant Finder site removes the burden, making it easy for everyone to pose and test alternatives within a global framework. We have a new laboratory for exploring high precision physics.

Appendix: Background on the Fundamental Constants

4.1. Planck's Constant, A Reference Value

In (Hartree) atomic units $\hbar = e = m_e = 4\pi\epsilon_0 = 1$. The speed of light is $1/\alpha \sim 137$. While convenient for some calculations, the unit system cannot be compared directly to experimental data, because it lacks a dimensionful scale. In "natural" units $\hbar = c = 1$ the masses have units of frequency. Calculations can be compared to data, where energy has units of frequency. Since frequency is the most precisely measured physical quantity, and directly measured in spectroscopy, the intermediate step of converting calculations to MKS energy with Planck's constant is bypassed. It is always possible to make the conversion, of course, but there is nothing fundamental to gain by expressing quantities in the units of Newtonian physics.

An efficient way to show that no high-precision measurements demand Planck's constant comes from the path integral. The weight of any quantum configuration is $e^{\imath S/\hbar}$, where S is the configuration's action. In the semi-classical old quantum theory the action of a classical particle in MKS units was used. In QED and the Standard Model we use the action of the quantum fields. The action in MKS units is multiplied by $\hbar$, which cancels out. The path integral is not a separate postulate, but derived from the time evolution operator $e^{-\imath Ht/\hbar}$. Then $H/\hbar$ and $S/\hbar$ are the relevant quantities, not H or S and $\hbar$ separately, and $\hbar$ cancels out.

In the Dirac sector, for example, the MKS mass term in natural units is $m_{MKS}\bar{\psi}\psi$, where ψ is the Dirac field. Then $m_{MKS}/\hbar$ appears in physical quantities, explaining why precision constants use the directly measured quantum of circulation $h/2m_e$ without dealing with the Newtonian electron mass and h separately. The textbook Dirac kinetic energy $\imath\hbar\bar{\psi}\partial_\mu\gamma^\mu\psi$ becomes $\imath\bar{\psi}\partial_\mu\gamma^\mu\psi$ in $S/\hbar$, so the time evolution is calculated directly in terms of frequency, bypassing Planck's constant.

The international organization charged with standardizing units plans in 2018 to set Planck's constant to a reference value[25], much as c was set to a reference value in 1983. The movement is connected with plans to eliminate the prototype kilogram as a standard. Since $\hbar$ is an MKS constant, any method to measure it must somewhere introduce the kilogram. A leading technology for a new standard is the watt-balance. It is a highly precise MKS device: As Ref. [3] writes, "By comparing mechanical power measured in terms of the meter, kilogram, and second to electrical power measured in terms of the Josephson and quantum Hall effects, watt-balance experiments have provided the best value for the Planck constant h." While setting Planck's constant to a reference value will make its role in precision physics more transparent, the current situation already has no fundamental role for $\hbar$.

4.2. The Electron Mass, or Compton Scale

As mentioned earlier the definition of the kilogram cancels out in $\lambda_e \sim h/m_{MKS}$. Compton's original scattering experiment directly observed the incoming and outgoing x-ray wavelengths with refraction off a crystal. This is why the experiment observed the Compton wavelength directly. The current experiments that measure the Compton scale also involve momentum conservation, as follows.

A collection of cooled atoms is trapped in an optical comb, which is a device using interference of laser beams to make an atomic trap. Lasers manipulate the atomic state of the atoms, which are typically ^{133}Cesium or ^{87}Rubidium. The trap is then adjusted to give the atoms a known velocity $\vec{v}$. The atoms collide with a laser beam of precisely known wave number $\vec{k}$. Momentum conservation $m_{MKS-atom}\vec{v} = N_\gamma \hbar k$. Knowing $\vec{v}$ and the number of photons N_γ allows $m_{MKS-atom}/\hbar$ to be measured.

Between 2008 and 2011 the relative uncertainty of $m_{MKS-Rb}/\hbar$ reported by the LKB group evolved from 9.2×10^{-9} to 1.9×10^{-9}, a factor of 7. While this is an impressive technical achievement, it is not very well documented. The best measurement[26] is described in a 4-page Physical Review Letter containing few details, and another paper for a popular audience[27]. While classical physics assumes classical physics is exact, the systematic errors of the theory used in the paper are not reported. Thus for many years an order of magnitude revision of an important experimental quantity has been poorly supported. Finally in 2017 new experiments emerged[28, 29].

Measuring one mass precisely determines many others because the atomic relative masses (relative to ^{12}C) are known with high precision, typically by using one apparatus for more than one measurement. Then measuring h/m_{Rb} with a known uncertainty measures h/m_e with a computable uncertainty. As Bouchendira et al. [26] relate it, a value for the fine structure constant can determined using

$$\alpha^2 = \frac{2R_\infty}{c}\frac{m_{Rb}}{m_e}\frac{h}{m_{Rb}}. \tag{5}$$

In that paper the relative errors on m_{Rb}/m_e and R_∞ were 7×10^{-12} and 4.4×10^{-10}, so that $\alpha^{-1} = 137035999037(91)$ was determined in one step with relative error 6.6×10^{-10}. Actually this kind of determination is circular, like the others, while it becomes meaningful in comparison with (say) α from $g-2$ or global fits. Our code includes a term $\chi^2_\lambda = (4\pi c R_\infty/\alpha^2 - (m_e/h)^{exp})^2/\sigma^2(m_e/h)$ which can be modified as desired, and where $\sigma^2(m_e/h)$ can be adjusted to any value.

4.3. The Electron Anomalous Moment Parameter

The Dirac Lagrangian defining the anomalous moment is $-\frac{\imath\kappa}{2m}\bar{\psi}\sigma_{\mu\nu}\psi F^{\mu\nu}$. The magnetic moment $\mu = ge/2m$ depends on the mass, while the moment parameter $a = (g-2)/2$ is dimensionless. The most precise measurements have been made in devices related to Penning traps. An electron in a magnetic field has a spin precession frequency ν_s and a cyclotron frequency ν_c. The solution to the Dirac equation predicts

$$\frac{g}{2} = 1 + \frac{\nu_s - \nu_c}{\nu_c} = 1 + \frac{\nu_a}{\nu_c},$$

where $\nu_a = \nu_s - \nu_c$ is called the anomaly frequency. The fact $g = 2$ in the zeroth order theory causes the series expansion of a_e to begin at $\alpha/2\pi \sim 1.12 \times 10^{-3}$, which is already a very small value. Due to the factor of 1000, observing a_e to an absolute precision of 10^{-9} determines g_e to relative precision of order 10^{12} (ppt). The fact the frequencies can then be observed in the same apparatus while integrating over relatively long times has made the electron's parameter a_e one of the most precisely measured numbers in physics.

As discussed in Ref. [30], the precision of recent measurements is actually sensitive to tiny relativistic effects. The lowest quantized energy levels with quantum numbers n, m_s are

$$E_{n,m_s} = \frac{g}{2} h\nu_c m_s + h(n + \frac{1}{2})\bar{\nu}_c - h\delta(n + \frac{1}{2} + m_s)^2.$$

Here $\bar{\nu}_c$ is a combination of frequencies more readily observed than ν_c, and δ is a relativistic correction, cited as

$$\delta = h\nu_c^2/mc^2 \sim 10^{-9}.$$

Once again the frequencies are observed without actual reference to Planck's constant. The 2011 determination of $g - 2$ to 0.28 ppt found

$$a_e = 0.00115965218073 \pm 2.8 \times 10^{-13}. \tag{6}$$

The *total* experimental uncertainty is much less than the relativistic correction.

The current Standard Model [31] calculation of the electron anomalous moment parameter is summarized by

$$a_e^{theory-QED} = 1.7147 \times 10^{-12} + 0.159155\alpha - 0.0332818\alpha^2 + 0.0380966\alpha^3$$
$$- 0.0196046\alpha^4 + 0.0299202\alpha^5. \tag{7}$$

The term of order 10^{-12} is the one-loop electroweak contribution plus hadronic contributions. Comparing Eq. 7 with Eq. 6 yields a value for α, along with a reference value for its uncertainty from the experimental uncertainty:

$$\begin{aligned}&1.7147\times10^{-12}+0.159155\alpha-0.0332818\alpha^2+0.0380966\alpha^3\\&-0.0196046\alpha^4+0.0299202\alpha^5-0.00115965218073=0;\\&\alpha\to\{1.091\pm1.106i,\,0.007,\,-0.767\pm1.270i\}.\end{aligned}\tag{8}$$

With more precision $\alpha = 0.0072973525644(17)$, and $\alpha^{-1} = 137.035999084(51)$. This is an example of *not* using a global fit, which at most determines a constant circularly. One can compare $\alpha^{-1} = 137.035999084(51)$ cited in Eq. 67 of Ref. [30].

The most cited published determinations of α are straightforward in arriving at the same result. While many possible inputs to determining the parameter are discussed, the least squares fits are strongly dominated by the smallest reported experimental uncertainty, which comes with a_e. Only one theoretical calculation of a_e to the claimed precision at order α^5 has been done. Near 2007 at least three errors (sometimes described as "an error") were found in the α^4 terms. While the errors were known before publishing the C06 review, they occurred after the rigid cut-off date for new information used by the review. Finally in 2010 the changes were incorporated, with the statement "the 2010 value of α shifted significantly and now is larger than the 2006 value by 6.5 times the uncertainty of that value." The variations in Figure 2 come from the published tables. They can also be reproduced simply by putting the *experimental* uncertainties in the evolving theory formulas, with no other information. The statistics of the fluctuations are not predicted by any of the estimated uncertainties appearing in the literature.

The exercise invites one to experiment. Dropping the term of order α^5 changes α by 3.9×10^{-12}. It also discovers another[14] real root $\alpha \sim 1.332$. Dropping the electroweak term decreases α by 1.08×10^{-11}. Considering alternatives, the one loop correction of a scalar particle with electron coupling constant α_X and mass m_X is

$$a_e^{theory-X} = 0.027706\,\xi m_X^2 f(m_X/m_\ell), \tag{9}$$

$$\text{where}\quad \xi = \frac{\alpha_X}{m_X^2} \tag{10}$$

[14]A polynomial of nth degree has n complex roots. We find no particular reason to omit multiple solutions.

Here m_ℓ is the lepton mass and $f(m_X/m_\ell)$ is an integral expression from the one-loop calculation found in the literature[32]. In the limit $m_X/m_\ell >> 1$ then $f \to 1$.

It is very easy to use the formula above with a nominal uncertainty to put a limit on Model-X-type parameters. However it is not globally consistent: The contribution of $a_e^{theory-X}$ changes the value of α. Moreover, it changes the value *trivially fit*, testing nothing, and the *sum of the two contributions is completely degenerate and indeterminate for the separate parts.* Considering the next-most precise determination of α is reasonable, but also not definitive: How does that experiment depend on theory assumptions? Why put very much attention on one experiment at all? Once again decisions are needed. It is not generally possible to set limits on new interactions, nor find the true (testable) uncertainties of QED theory without incorporating maximal experimental information using global fits.

4.4. The Muon Anomalous Moment Parameter

The muon is much different from the electron, in both theory and experiment. Due to the muon's mass the contribution of hadronic physics is significant. The one-loop hadronic vacuum polarization contribution is non-perturbative, and depends on fitting experimental data. The experimentally-deduced hadronic vacuum polarization is significant, the "light-by-light" contribution is controversial, and the electroweak contributions are much different from the electrons. Collecting the terms of Ref. [33] gives the muon anomalous moment parameter a_μ

$$a_\mu = 2.7 \times 10^{-9} + 0.15155\alpha + .0788406\alpha^2 + 0.77665\alpha^3 + 1.3436\alpha^4 + 2.4616\alpha^5 \tag{11}$$

The parameter is measured by a technique conceptually similar to the Penning-trap measurements: The critical observable is the difference between the spin and rotational frequencies. However the regime is a high energy one using a *classical* equation of motion. The classical spin is a spacelike 4-vector s_μ normalized to $s^2 = -1$ and orthogonal to the classical 4-momentum p_μ. The magnetic moment associated with a spin precesses in a magnetic field. When a muon decays by $\mu \to e + \nu_\mu + \bar{\nu}_e$ the final state electron's angular distribution is correlated with the muon spin. The experiment observes an oscillating time dependence of final state electrons from muons circulating in a precisely determined magnetic field.

The so-called BMT equation for the spin plays a critical role. Some derivations are difficult, so we present a short one here. Differentiating gives $s' \cdot p + s \cdot p' = 0$, where prime is the derivative with respect to proper time τ. Multiply by s and contract, and then $s' \cdot p = -s \cdot f$ is *pre-determined* by the relativistic force f. The non-trivial spin equation must predict the perpendicular part,

$$(g_{\mu\nu} - p_\mu p_\nu/m^2)\frac{ds^\nu}{d\tau} = \Omega_\mu, \frac{ds_\mu}{d\tau} + u_\mu s \cdot u' = \Omega_\mu; \qquad p_\mu = mu_\mu.$$

The $u_\mu u' \cdot s$ term on the left side is the Thomas precession. If the only interaction comes from an external field $\mathcal{F}_{\mu\nu}$, the only 4-vectors linear in s are $u_\mu s^\alpha \mathcal{F}_{\alpha\beta} u^\beta$ and $\mathcal{F}_{\mu\beta} s^\beta$. The most general equation is

$$\frac{ds_\mu}{d\tau} = -u_\mu s \cdot u' + \frac{\alpha}{m_C} u_\mu s^\alpha \mathcal{F}_{\alpha\beta} u^\beta + \frac{\beta}{m_C} \mathcal{F}_{\mu\beta} s^\beta.$$

This is the BMT equation before assuming the classical Lorentz force, $p'_\mu = e_{MKS} F_{\mu\nu} u_\nu$. With that assumption and identifying parameters in the non-relativistic limit gives

$$\frac{d\vec{s}}{dt} = (\frac{\alpha}{m_C} - e_{MKS})\vec{v}(\vec{s} \cdot (\vec{v} \times \vec{B})) + \frac{\beta}{m_C}(\vec{s} \times \vec{B}) \approx \frac{\beta}{m_C}(\vec{s} \times \vec{B}), \quad (12)$$

where in the last step we have assumed $v/c << 1$. In terms of background magnetic and electric fields $\vec{B}$, $\vec{E}$ the anomalous spin precession frequency is

$$\vec{\omega}_a = \vec{\omega}_s - \vec{\omega}_c = -\frac{e_{MKS}}{m_{\mu MKS}}(a_\mu \vec{B} - (a_\mu - \frac{1}{\gamma^2 - 1}\beta \times \vec{E})). \quad (13)$$

This assumes the spin and velocity vectors are orthogonal to the magnetic field. The dependence of a_μ on the electric field is minimized by storing muons with the "magic " boost factor $\gamma = 29.3$, equivalent to a muon momentum $p = 3.09$ GeV/c. Then B and $e_{MKS}/m_{\mu MKS}$ need to be known to determine a_μ from ω_a. The scale $e_{MKS}/m_{\mu MKS}$ is conventionally eliminated in terms of $\mu_\mu/\mu_p = 3.18334539(10)$[34]. The number and uncertainty in μ_μ/μ_p depends on more theory and experiments given in the references.

The Brookhaven E821 experiment [5] found $a_\mu = 0.00116592091(63)$. This value is larger than calculations by 2.9×10^{-9}, which is nominally 3.9σ. The muon ring has been moved to Fermilab, where a new experiment is underway. The muon's moment is an arena where theoretical alternatives using Eq. 9

have been extensively explored[35, 36, 37, 38, 39, 40, 41, 42]. Note, however, that when analysis fixes other fundamental constants such as α and μ_μ/μ_p, the piecemeal exploration will be limited to those assumptions, and generally produce outcomes that are overly restrictive.

4.5. The Rydberg Constant

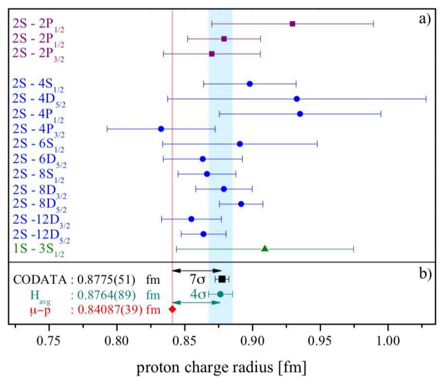

Figure 1. a) The proton charge radius obtained from precision spectroscopy of atomic hydrogen. Either radio frequency measurements of the 2S-2P Lamb shift (violet) or optical transition frequencies (blue from the 2S and green from the 1S state) are used. To extract the two parameters, the Rydberg constant and the proton charge radius, each of these measurements needs to be combined with another independent measurement, which is the 1S-2S transition frequency here. b) The analysis reveals a 4σ discrepancy between the hydrogen mean value (H_{avg}) and the value determined from laser spectroscopy of muonic hydrogen (μ–p). An even larger inconsistency of 7σ is obtained when including proton-electron scattering data. This CODATA analysis also uses deuterium data, that have only limited effect on the proton charge radius, because its nucleus is not a proton. A similar picture is obtained when plotting the corresponding results for the Rydberg constant.

Figure 12. One approach to fitting the proton charge radius from Ref. [21], along with its caption.

The energies of the bound hydrogen atomic states with quantum number n are -13.6 eV/n^2. Atomic physicists re-arrange the perturbative theory of the atom to maintain the Rydberg constant[15] $R_\infty = \alpha^2 m_e/2$ as the fundamental scale. Highly precise atomic transition frequencies will determine R_∞ to a better precision than computing it with typical uncertainties of α and λ_e, *provided*

[15] In natural units

they and the proton or deuteron charge radius is known with sufficient precision. The charge radius of the proton r_p enters from an expansion of its electromagnetic form factor in powers of momentum transfer q^2:

$$F_1(q^{2)} = 1 - 6r_p^2 q^2 + O(q^4).$$

Section 4.6 defines F_1. The deuteron charge radius analog enters with atomic deuterium data.

With the other parameters fixed, two transition frequencies of atomic hydrogen can be fit to two values of R_∞ and r_p. Figure 12 shows the results from Ref. [21]. We reproduced this calculation, along with its error bars, which come from simply adding and subtracting the experimental uncertainties of the transitions shown. The other transition for each case is the $1S2S$, whose experimental uncertainty of 10 Hz is hundreds to thousands of times smaller than all the others. It is widely believed that such multiple two-parameter fits determine the Rydberg at highest possible precision, and that the process depends critically on the superb experimental measurement of the $1S2S$ frequency. Neither belief is true.

It is also believed that theory reproducing the $1S2S$ transition is very demanding, and a supreme test of the theory. Yet actually nothing is tested. Using one ultra-precise datum forces the entire analysis to conform to one ultra-precise datum. The comparison of theory predictions and experimental values in Table 1 of Ref. [43] shows *exact* agreement of experiment and theory and their uncertainties in the first line. About this A. Kramida[22] has remarked:

> However, one thing can be stated with certainty: the exact agreement of those two ultra-precise $1S2S$ measurements with the QED calculations cannot be considered as a confirmation of the QED theory, because it is the result of the fitting of the fundamental constants based on these (and other) transitions.

In fact the $1S2S$ transition is *185 times more precise than the next most precise transition*. The ratio of the smallest to the mean σ_i^2 in the data set used is 34225. Any datum with uncertainties much smaller than all the others will completely dominate a basic least-squares fit using experimental denominators σ_{exp}^2. The demands of fitting the $1S2S$ transition with great exactness and *without considering a single further item of experimental or theoretical information* are expressed with a linear relation between two parameters:

$$r_p \sim 0.877{+}1.05 \times 10^9 \delta R_\infty / R_\infty^\bullet, \tag{14}$$

assuming $10^9\delta R_\infty/R_\infty^\bullet << 1$. Here r_p is in units of Fermi, and $R_\infty = R_\infty^\bullet(1+\delta R_\infty/R_\infty^\bullet)$, where $R_\infty^\bullet$ is a reference value of 1097331.568539 m^{-1} The symbol δR_∞ can be called "the offset" relative to the reference value to avoid confusion with the fitting uncertainty of R_∞.

Eq. 14 will be called the "$1S2S$ degeneracy line". A similar degeneracy line exists for each transition, but their uncertainties are so much larger that none dominate a global fit. Eq. 14 has been evaluated using the C10 reference value and the group's choice of electron scattering data. The data from muonic hydrogen $r_p \sim 0.84$ has been excluded. That decision yields $r_p = 0.877$ at $\delta R_\infty = 0$. On the other hand choosing $r_p = 0.84$ gives $\delta R_\infty/R_\infty^\bullet = 9.5 \times 10^{-10}$. (There is a strong case that $r_p = 0.84$ is the more reliable value, as discussed in Section 4.6.) See Figure 1 for estimated uncertainties.

A few facts explain why the $1S2S$ line can be measured with great precision. It is a 2-photon transition with a very long lifetime and correspondingly small natural line width. The experiment excites the transition with two photons, cancelling Doppler recoil effects. And the scientists are experimental geniuses who rightly deserve the Nobel Prize awarded in 1997. As a consequence, few doubt the importance of the $1S2S$ transition for determining the fundamental constants. Yet so far in this discussion something has been overlooked. Fundamental constants depend on the theory used to evaluate them. The theoretical uncertainty σ_{theory} of the $1S2S$ transition is *much larger* than its experimental uncertainty. Estimates in the literature vary, with $\sigma_{theory} \sim 10^4$Hz the order of magnitude, and $\sigma_{theory} \sim 2.5\times^3$Hz the smallest value we have seen. How does one assess the usefulness of an experimental number whose theoretical uncertainty is 250-1000 times larger than its experimental one?

C10 and C18[44] use a version of χ^2 with pull to treat theory uncertainties with additive constants. Table XVIII of C10 shows 52 "principal input data for the determination of the 2010 recommended value of the Rydberg constant R_∞". Of the 52 input data 27 entries are experimental data. These data are 16 values of selected hydrogen transition frequencies, plus 8 deuterium transition frequencies, along with two values of the proton radius r_p and one deuteron charge radius analog r_d from electron scattering. The other 25 *input data* are the initial values of pull parameters ("additive corrections ") $\delta_H(1S_{1/2})$, $\delta_H(2S_{1/2})$, etc. Those input data are varied in the fit to become outputs. (It is characteristic of χ^2 with pull to have more free parameters than experimental data.) The estimated theory errors appear in the denominators of pull parameters. When the theory uncertainty assigned to the $1S2S$ is sufficiently small, then R_∞ and

r_p are guaranteed to lie along a certain $1S2S$ degeneracy line, regardless of what theory is used.

Reconsidering Figure 12, suppose the theory used for the $1S2S$ transition is modified by adding a constant Δf_{1S2S}. Then since the points are all determined relative to a $1S2S$ baseline, the central value of every point shifts to the right or left by a calculable amount. The uncertainties are even more interesting. The smallest experimental uncertainty after the $1S2S$ is 6396Hz. A theoretical uncertainty of order 10^4 Hz added in quadrature will more than double the size of all the error bars in the upper part of Figure 12. There seems to be two reasons this has been overlooked. First, there is a perception in atomic physics that theory is already much more precise than experiment. It is generally true, *except* for the $1S$ level, which is particularly difficult to calculate and sensitive to calculations that (in fact) are incomplete. Second, the acclaim for the $1S2S$ experiment has sometimes forgotten the role of theory, in an experimental world-view where the fundamental constants might have been self-defining quantities.

Figure 13 shows an experiment fitting R_∞ and r_{p-eH} while entirely removing the $1S2S$ transition. The analysis uses the standard set of transitions in a basic least squares fit with no pull parameters or correlations and experimental uncertainties[16], and again ignores the muonic hydrogen data for $r_{p-\mu H}$. The uncertainty in R_∞ shown is about twice as large as when using the $1S2S$ with a χ^2-pull theory uncertainty of 2.5kHz. That decision is responsible for the reported error bars on R_∞. If the theory uncertainty is much smaller, the error bars on R_∞ will decrease. If the theory uncertainty is much larger, the $1S2S$ has less and less weight, until its effects are the same as removing it altogether.

The figure shows the perception that the proton size has been precisely and unconditionally determined by spectroscopy is flawed. The spectroscopic data actually determines a *correlation* between two free parameters, which are r_{p-eH} and R_∞. The correlation coefficient of C10 fits is 0.99, meaning that r_{p-eH} and R_∞ can be varied quite a bit along a straight line while giving a good fit. It is a basic concept error to use error bars without attending to such correlations.

What is to be made of the great sensitivity of the Rydberg constant to procedural decisions? We think it's important to know the sensitivity to procedure exists. The amount of sensitivity is adjustable: The role of R_∞ as "the most precisely determined physical constant" is somewhat of a sociological agreement.

[16]Results do not change significantly when the published experimental correlations are included.

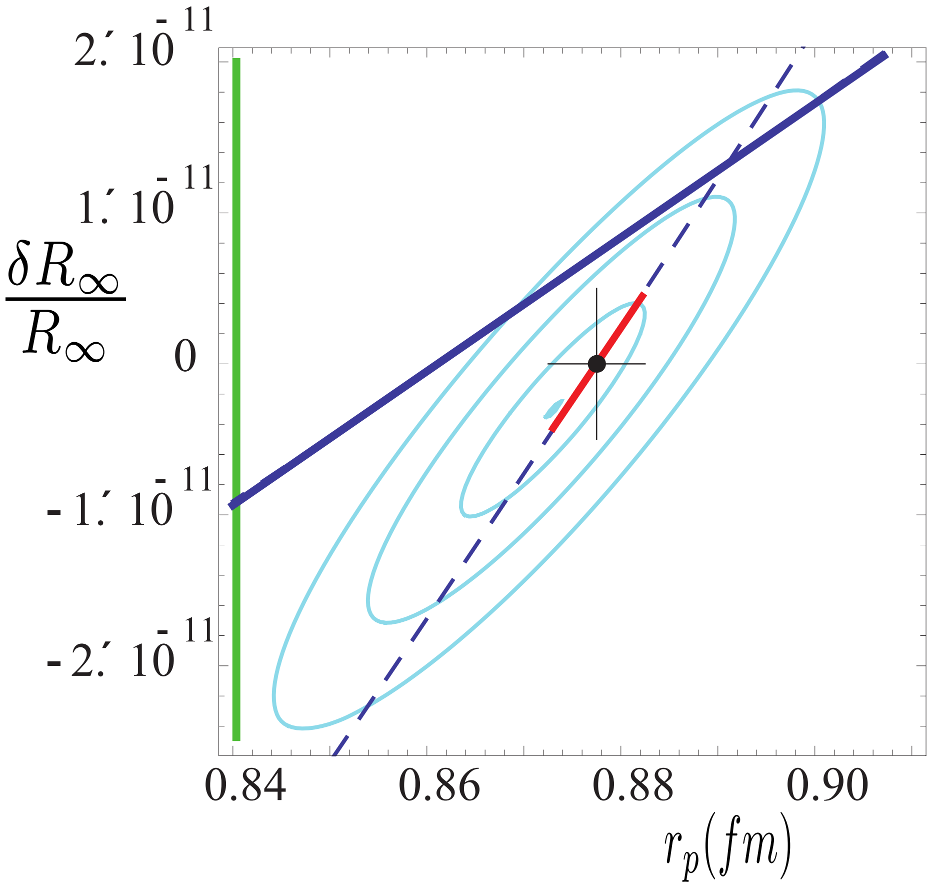

Figure 13. Contours or "error ellipses" of χ^2 in the $(r_p,\ \delta R_\infty/R_\infty)$ plane) with the $1S2S$ transition omitted for a fit to eH spectroscopic data. Contours show 1, 2, 3 σ Gaussian confidence levels corresponding to $\Delta\chi^2$ = 1, 4, 9. The muonic value $r_p = 0.841$ fm is at the left edge of the plot close to the 3σ contour. Including the $1S2S$ transition produces a 1σ error ellipse too thin to resolve graphically, and represented by the thick segment (red online). The dashed line is the degeneracy line of the $1S2S$ transition. Least-squares analysis dominated by this single datum predicts r_p and R_∞ fall on the line, regardless of other data or theory. The point and its error bars are the values published by C10[6], which are predicted to lie along the line. The next most precise transition produces a different degeneracy line (solid line), which barely intersects the 2σ region.

In general, the uncertainty of the Rydberg can be increased without causing undue effects in the global relations between constants. How much one will allow deviating from previous determinations is a subjective issue.

4.6. The Proton and Deuteron Charge Radii

The coupling of a spin-1/2 particle to a virtual photon is parameterized by form factors, defined by

$$< p's'|J_\mu|ps >= \bar{u}(p',\, s')\left(e\gamma_\mu F_1(q^{2)} + \frac{\imath e}{2m}\sigma_{\mu\nu}q^\nu F_2(q^2)\right)u(p,\, s)$$

where $q^\nu = (p' - p)^\nu$, $q^2 = q_\mu q^\mu$, and the other symbols are defined in textbooks[45]. The proton charge radius is *defined* by

$$r_p^2 = -6\frac{\partial G_E}{\partial q^2}\Big|_{q^2=0}, \tag{15}$$

where $G_E = F_1 + q^2 F_2/4m^2$. The name "charge radius" is not directly related to the quantity measured.

The name originally came from non-relativistic, Born-level perturbation theory, a procedure not suited to definitions, and not currently relevant. It can also be motivated by a model superposing relativistic scattering amplitudes with momentum transfer $\vec{q}$ over a static, non-dynamical spatial charge distribution. That leads to a picture where $F_1(\vec{q})$ is the Fourier transform of the spatial charge distribution, with a second moment given by the derivative. The actual scattering of a photon with relativistic quarks and antiquarks in a proton is highly dynamical: the system reacts with the probe, and can hardly be "undisturbed". Moreover, both sides of Eq. 15 are Lorentz scalars. The second moment of a charge density transforms differently, like a 3-vector-squared. Thus r_p is not exactly the proton charge radius, but the terminology does not matter so long as the quantity is used consistently, and the misnomer does not affect further calculations...which it sometimes does[17].

Estimates of r_p from electron scattering have a very long history going back to Rutherford. The q^2 dependence of F_1 has been measured many times by many different groups often with remarkable precision. However the scattering

[17]The definition $r_p^2 = \int d^3x\, r^2 \rho_E(r)$ is sometimes cited when the derivative of F_1 is actually used. When the density-based definition is imposed in analysis of F_1 it can introduce an unphysical bias.

cross section at $q^2 = 0$ is singular, and $\partial F_1/\partial q^2\big|_{q^2=0}$ is unobservable in scattering. It is estimated from scattering data by extrapolation. For the purpose of determining the other fundamental constants the extrapolation need not reproduce $q^2 = 0$ exactly, but approach the atomic physics scale of q^2 comparable to R_∞^{-2}. That is quite difficult.

The process of extrapolation is controversial. It is easy to convince oneself that $0.8 < r_p < 0.9$, while 2-digit precision depends on decisions. A fit from Mergell called "a comprehensive analysis " gave $r_p = 0.84$ fm and was used in the C98 report. Curiously this value coincides with the determination from muonic hydrogen, discussed in a moment. Subsequently C02 and later reports abandoned that value in favor of values of $r_p \sim 0.89$, for which the analysis of [46] has been cited. The reason for the choice is that different values of r_p degrade the determination of the Rydberg. Meanwhile, renewed interest in extrapolation sensitivity has yielded several papers[47, 48] showing that existing electron scattering data is incapable of distinguishing $r_p \sim 0.84$ from $r_p \sim 0.9$. The PRAD experiment[19] has been underway, and will attempt to measure the form factor at 1% accuracy down to the region of $q^2 \sim 10^{-4}\, GeV^2$.

The *proton size puzzle* refers to a perceived inconsistency of r_{pe} extracted from electron scattering, and $r_{p\mu H}$ extracted from muonic hydrogen spectroscopy. Many explanations have been proposed[49, 50, 51, 52, 53]. The Lamb shift calculations of muonic hydrogen are remarkably simple compared to electronic hydrogen[54]. The contribution of r_p scales like the wave function squared at the origin. Due to the muon mass $m_\mu \sim 207 m_e$, the effects of $r_{p\mu H}$ are $207^3 \sim 10^7$ times larger in μH than in eH. The proton size then makes a relatively large and observable contribution in μH, where[55] the $2S_{F=0} - 2P_{F=1}$ energy difference in units of meV is

$$\Delta E(\alpha,\, r_{p\mu H}) = 0.0332 + 206.0336\alpha^3/\alpha_\bullet^3 - 5.2275 r_{p\mu H}^2 \alpha^4/\alpha_\bullet^4 \qquad (16)$$

The CREMA collaboration(Antognini et al 2013)[55] measured $r_{p\mu H} = 0.84087(39)$. This value was subsequently confirmed with an improved apparatus. The experiment cleverly measures a line in a nearly ideal experimental regime. It is in close conjunction with well-known water absorption lines that directly calibrate the laser frequency. It also directly observes the resonance in the spectra of electrons from muon decay. The simplicity and quality of the experiment and its theory make a strong case that the *parameter* measured in μH is the most reliable measurement of "the proton size."

The muonic deuterium charge radius $r_{p\mu D}$ is a powerful consistency check[18]. Pohl et al[2] mention the isotope shift of the $1S2S$ transition[19] and its determination of $r^2_{peD} - r^2_{peH} = 3.82007(65)\,fm^2$ to very high precision. Replacing $r_{peH} \rightarrow r_{p\mu H}$ predicts $r_{peD} = 2.12809(31)$. This is quite compatible with $2.1286(93)$ from adjustment 11 from Table XLV of C06, which is the final fitting method using only deuterium data. However the high precision of the difference ties r_{peD} and r_{peH} together. Then the C06 final value of $r_{peD} = 2.1402(28)$ is 4.1σ away from its own deuteron-based determination. Since that time, CREMA[13] has measured the Lamb shift in muonic deuterium directly, obtaining $r_{\mu D} = 2.12562(78)$, which is consistent with its own findings. Due to effects disturbing the global fits C10 and C14 do not use the μH or μD data, which is quite justified given their stated objective.

As Ref. [2] discusses, the multiple 2-parameter fits (Figure 12) produce a value $R_\infty(\mu H) = 10973731.568160(16)\,m^{-1}$, whose central value disagrees with C10 by 4.9σ. But that does not mean that every analysis would revise R_∞ by the same amount when using $r_{p\mu H}$. Everything depends on the analysis method, the data selected for the comparison, and the theory. Just as with the anomalous moments, the contribution of new physics causes a degeneracy in fitting parameters. The formula[56] is

$$\Delta E_{tot}(\alpha,\, r_{p\mu H},\, \alpha_X\; m_X,\, m_{red}) \\ = \Delta E(\alpha,\, r_{p\mu H}) + +10^9(m_X^4 \xi)/(2\alpha m_{red}(1 + m_X/(\alpha m_{red}))^4), \qquad (17)$$

where m_{red} is the reduced mass of the atom. Observing a given value for ΔE_{tot} cannot determine $r_{p\mu H}$ or the X-contribution separately, but only the sum shown. The MUSE experiment seeks to measure μp scattering at low momentum transfer, which will contribute more information, especially if there is a new muon-specific interaction.

4.7. Theoretical Uncertainties: The Wild Card

There are no universal rules for incorporating estimated theory uncertainties in data analysis. Barlow[57] has explained theory uncertainty is an intrinsically Bayesian issue. For example, the method called “chi-squared with pull” (Eq. 2)

[18] While muonic atoms with larger nuclei beginning with He^3 are fascinating, the uncertainties of nuclear theory quickly become problematic for using such measurements to resolve the proton size problem.

[19] Most of the theoretical uncertainties inherent in the $1S2S$ cancel in the isotope shift.

adds new parameters δ_j to the theory and assumes the δ_j are normally distributed about zero with estimated uncertainties $\sigma^2_{\delta_j}$. The results then depend on σ_{δ_j}, which are essentially free parameters representing one?s belief in the theory.

The Appendix of Ref. [58] reviews this and warns that fitted outputs can be unexpectedly sensitive to the σ_{δ_j}. The method tends to punish high confidence in theory, and reward low confidence, somewhat counter-intuitively. If the theory is not trusted, then σ_{δ_j} are large, allowing the additive parameters to shift the theory and fit the data better. However the range of theory parameters fitting within a given confidence level is also increased, downgrading parameter resolution. High confidence in theory is represented by small σ_{δ_j} that prevents additive parameters from helping the theory. Like all Bayesian procedures the results depend on one's beliefs about the theoretical uncertainties σ_{δ_j}, known as priors. The process of fitting the δ_j can be bypassed (in Bayesian terms, concealed) if one marginalizes over the distribution of priors. For a normal distribution that replaces $\sigma^2_{exp-i} \to \sigma^2_{exp-i} + \sigma^2_{\delta-i}$ in the denominators of χ^2. Add theory and experimental errors in quadrature. The formula automates a rule that if theory uncertainties are sufficiently small compared to experimental ones, they have no effect.

Almost by definition, theoretical uncertainties must be smaller than experimental ones to discover experimental anomalies. (When the opposite happens, the theory is inadequate to confront the data, and discrepancies do not become anomalies.) The decision that anomalies exist takes as a starting point that theory errors are not the leading candidate for explanation. As consistent, almost all of the data and theory elements of our study have been repeatedly examined to rule out an important role for theoretical uncertainty, or avoid it when present.

For example, the theory of the muonic Lamb shift[59] is beautifully simple, compared to the electronic Lamb shift. The proton size contribution is ten million times larger than in electronic hydrogen, and almost all of it comes from first order perturbation theory. The muonic Lamb shift is theoretically robust, and calculations are complete. Higher order corrections make small contributions, and they have been calculated from first principles.

The theory of the electron anomalous moment is quite difficult. It has only been computed to the highest precision by one group. We are in no place to criticize this tremendous body of work. Yet significant mistakes have been found in the past. We have no insight to estimate the theoretical uncertainty.

The theory of electronic hydrogen and deuterium is extremely complicated. The estimated theoretical uncertainties of $\alpha log \alpha$ series expansions do not always agree with calculations done after the estimates. Higher order terms are not reliably of order α/π relative to lower order ones. Instead they tend to be much larger, so that theory uncertainties are routinely underestimated. Almost all of the electronic hydrogen and deuterium spectra are all fit to within a fraction of the experimental uncertainty with $\chi^2/dof < 1$. That is evidence that theory uncertainty is not larger than the experimental uncertainties. It is not evidence for smaller theory uncertainties that are sometimes estimated.

In summary, any method increasing theory uncertainty makes fitting data and explaining experimental anomalies easier. It improves fits by decreasing χ^2 while decreasing parameter resolution. Conversely, a goal to minimize uncertainties on fitted parameters automatically chooses to minimize theoretical uncertainties. How to assess theory uncertainties is ultimately a procedural decision. Exploring the effects of theory uncertainties is one of the reasons the Constant Finder site exists.

References

[1] Pohl R., Antognini A., Nez F., Amaro F. D., Biraben F., *et al.*, "The size of the proton," *Nature*, vol. 466, p. 213, 2010.

[2] Pohl R., Antognini A., Amaro F., Biraben F., Cardoso J., Covita D., Dax A., Dhawan S., Diepold M., Fernandes L., Giesen A., Gouvea A., Graf T., Haensch T., Indelicato P., Julien L., Kao C.-Y., Knowles P., Matias-Lopes J., and Kottmann F., "Laser spectroscopy of muonic hydrogen," vol. 525, pp. 647–651, 09 2013.

[3] Mohr P. J., Taylor B. N., and Newell D. B., "The fundamental physical constants," *Phys. Today*, vol. 60N7, pp. 52–55, 2007.

[4] Karshenboim S. G., "Fundamental physical constants: looking from different angles," *Canadian Journal of Physics*, vol. 83, p. 767, Aug. 2005.

[5] Bennett G. W. *et al.*, "Measurement of the negative muon anomalous magnetic moment to 0.7 ppm," *Phys. Rev. Lett.*, vol. 92, p. 161802, 2004.

[6] Mohr P. J., Taylor B. N., and Newell D. B., "CODATA Recommended Values of the Fundamental Physical Constants: 2010," *Rev. Mod. Phys.*, vol. 84, p. 1527, 2012.

[7] Patrignani C. *et al.*, “Review of Particle Physics,” *Chin. Phys.*, vol. C40, no. 10, p. 100001, 2016.

[8] “NIST Reference on Constants, Units, and Uncertainties,” National Institute of Standards and Technology, Gaithersburg, MD 2012. [Online] https://physics.nist.gov/cuu/Constants/.

[9] Newton G., Andrews D. A., and Unsworth P. J., “A precision determination of the lamb shift in hydrogen,” *Philosophical Transactions of the Royal Society of London. Series A, Mathematical and Physical Sciences*, vol. 290, no. 1373, pp. 373–404, 1979.

[10] Lundeen S. R. and Pipkin F. M., “Separated oscillatory field measurement of the lamb shift in h, n = 2,” *Metrologia*, vol. 22, no. 1, p. 9, 1986.

[11] Hagley E. W. and Pipkin F. M., “Separated oscillatory field measurement of hydrogen $2s_{1/2}$-$2p_{3/2}$ fine structure interval,” *Phys. Rev. Lett.*, vol. 72, pp. 1172–1175, Feb 1994.

[12] Hanneke D., Fogwell Hoogerheide S., and Gabrielse G., “Cavity control of a single-electron quantum cyclotron: Measuring the electron magnetic moment,” *Phys. Rev. A*, vol. 83, p. 052122, May 2011.

[13] Pohl R. *et al.*, “Laser spectroscopy of muonic deuterium,” *Science*, vol. 353, no. 6300, pp. 669–673, 2016.

[14] Mohr P. J., Newell D. B., and Taylor B. N., “CODATA Recommended Values of the Fundamental Physical Constants: 2014,” *ArXiv e-prints*, 2015.

[15] Martens J. C. and Ralston J. P., “The Muon Experimental Anomalies Are Explained by a New Interaction Proportional to Charge,” 2016.

[16] Wolfram Research, Inc., “webMathematica, Version 3.4.” Champaign, IL, 2018.

[17] Horbatsch M. and Hessels E. A., “Evaluation of the strength of electron-proton scattering data for determining the proton charge radius,” *Phys. Rev.*, vol. C93, no. 1, p. 015204, 2016.

[18] “The MAMI Electron Scattering Program,” Johannes Gutenberg Universitat, Mainz, 2016. [Online] https://www.jlab.org/conferences/elba/talks/wednesday/morning_session/Schlimme.pdf.

[19] Peng C. and Gao H., "Proton Charge Radius (PRad) Experiment at Jefferson Lab," *EPJ Web Conf.*, vol. 113, p. 03007, 2016.

[20] Downie E. J., "The MUSE experiment," *EPJ Web Conf.*, vol. 73, p. 07005, 2014.

[21] Beyer A. *et al.*, "Precision Spectroscopy of Atomic Hydrogen," *J. Phys.: Conf. Ser.*, vol. 467, p. 012003, Dec. 2013.

[22] Kramida A. E., "A critical compilation of experimental data on spectral lines and energy levels of hydrogen, deuterium, and tritium," *At. Data Nucl. Data Tables*, vol. 96, p. 586, 2010.

[23] Jentschura U., Kotochigova S., Bigot E. L., Mohr P., and Taylor B., "The energy levels of hydrogen and deuterium (version 2.1)," National Institute of Standards and Technology, Gaithersburg, MD 2005. [Online] http://www.nist.gov/pml/data/hdel/index.cfm.

[24] Battaglieri M. *et al.*, "US Cosmic Visions: New Ideas in Dark Matter 2017: Community Report," 2017.

[25] "Draft Resolution A: On the revision of the International System of units (SI)," Bureau International des Poids et Mesures, Sevre, France, year = 2017, note = [Online] https://www.bipm.org/utils/en/pdf/CGPM/Draft-Resolution-A-EN.pdf.

[26] Bouchendira R., Cladé P., Guellati-Khélifa S., Nez F., and Biraben F., "New Determination of the Fine Structure Constant and Test of the Quantum Electrodynamics," *Physical Review Letters*, vol. 106, p. 080801, Feb. 2011.

[27] Bouchendira R., Cladé P., Guellati-Khélifa S., Nez F., and Biraben F., "State of the art in the determination of the fine structure constant: test of Quantum Electrodynamics and determination of h/m_u," *Annalen Phys.*, vol. 525, no. 7, pp. 484–492, 2013.

[28] Huang W., Audi G., Wang M., Kondev F., Naimi S., and Xu X., "The AME2016 atomic mass evaluation (I). Evaluation of input data; and adjustment procedures," *Chinese Physics C*, vol. 41, no. 3, p. 030002, 2017.

[29] Wang M., Audi G., Kondev F., Huang W., Naimi S., and Xu X., "The AME2016 atomic mass evaluation (II). Tables, graphs and references," *Chinese Physics C*, vol. 41, no. 3, p. 030003, 2017.

[30] "Trapped Positrons for High-Precision Magnetic Moment Measurements," S. Fogwell Hoogerheide, year = 2014, note = [Online] http://nrs.harvard.edu/urn-3:HUL.InstRepos:10985007.

[31] Aoyama T., Hayakawa M., Kinoshita T., and Nio M., "Tenth-Order Electron Anomalous Magnetic Moment — Contribution of Diagrams without Closed Lepton Loops," *Phys. Rev.*, vol. D91, no. 3, p. 033006, 2015.

[32] Leveille J. P., "The second-order weak correction to (g - 2) of the muon in arbitrary gauge models," *Nuclear Physics B*, vol. 137, pp. 63–76, 1978.

[33] Aoyama T., Hayakawa M., Kinoshita T., and Nio M., "Complete Tenth-Order QED Contribution to the Muon g-2," *Phys. Rev. Lett.*, vol. 109, p. 111808, 2012.

[34] Liu W. *et al.*, "High precision measurements of the ground state hyperfine structure interval of muonium and of the muon magnetic moment," *Phys. Rev. Lett.*, vol. 82, pp. 711–714, 1999.

[35] Kowalska K. and Sessolo E. M., "Expectations for the muon g-2 in simplified models with dark matter," *JHEP*, vol. 09, p. 112, 2017.

[36] Calibbi L., Ziegler R., and Zupan J., "Minimal Models for Dark Matter and the Muon g-2 Anomaly," 2018.

[37] Queiroz F. S. and Shepherd W., "New Physics Contributions to the Muon Anomalous Magnetic Moment: A Numerical Code," *Phys. Rev.*, vol. D89, no. 9, p. 095024, 2014.

[38] Biggio C., Bordone M., Di Luzio L., and Ridolfi G., "Massive vectors and loop observables: the $g - 2$ case," *JHEP*, vol. 10, p. 002, 2016.

[39] Pospelov M., "Secluded U(1) below the weak scale," *Phys. Rev.*, vol. D80, p. 095002, 2009.

[40] Gninenko S. and Krasnikov N., "Probing the muon $g_\mu - 2$ anomaly, $L_\mu - L_\tau$ gauge boson and dark matter in dark photon experiments," *Phys. Lett. B*, vol. B783, 2018.

[41] Karshenboim S. G., McKeen D., and Pospelov M., "Constraints on muon-specific dark forces," 2014.

[42] Tucker-Smith D. and Yavin I., "Muonic hydrogen and MeV forces," *Phys. Rev. D*, vol. D83, p. 101702, 2011.

[43] Jentschura U. D., Kotochigova S., Le Bigot E.-O., Mohr P. J., and Taylor B. N., "Precise Calculation of Transition Frequencies of Hydrogen and Deuterium Based on a Least-Squares Analysis," *Phys. Rev. Lett.*, vol. 95, p. 163003, Oct. 2005.

[44] Mohr P. J., Newell D. B., Taylor B. N., and Tiesinga E., "Data and analysis for the CODATA 2017 special fundamental constants adjustment," *Metrologia*, vol. 55, no. 1, p. 125, 2018.

[45] Peskin M. E. and Schroeder D. V., *An Introduction to quantum field theory*. Reading, USA: Addison-Wesley, 1995.

[46] Sick I., "On the RMS radius of the proton," *Phys. Lett. B*, vol. B576, p. 62, 2003.

[47] Higinbotham D. W., Kabir A. A., Lin V., Meekins D., Norum B., and Sawatzky B., "Proton radius from electron scattering data," *Phys. Rev.*, vol. C93, no. 5, p. 055207, 2016.

[48] Arrington J., "New measurements of the proton's size and structure using polarized photons," *AIP Conf. Proc.*, vol. 1560, p. 525, 2013.

[49] Carlson C. E., "The Proton Radius Puzzle," *Prog. Part. Nucl. Phys.*, vol. 82, pp. 59–77, 2015.

[50] Barger V., Chiang C.-W., Keung W.-Y., and Marfatia D., "Proton size anomaly," *Phys. Rev. Lett.*, vol. 106, p. 153001, 2011.

[51] De Rujula A., "QED is not endangered by the proton's size," *Phys. Lett. B*, vol. B693, p. 555, 2010.

[52] Hill R. J., "Review of Experimental and Theoretical Status of the Proton Radius Puzzle," *EPJ Web Conf.*, vol. 137, p. 01023, 2017.

[53] Cloet I. C. and Miller G. A., "Third Zemach Moment of the Proton," *Phys. Rev.*, vol. C83, p. 012201, 2011.

[54] Pohl R., Gilman R., Miller G. A., and Pachucki K., "Muonic hydrogen and the proton radius puzzle," *Ann. Rev. Nucl. Part. Sci.*, vol. 63, p. 175, 2013.

[55] Antognini A., Nez F., Schuhmann K., Amaro F. D., Biraben F., *et al.*, "Proton Structure from the Measurement of $2S - 2P$ Transition Frequencies of Muonic Hydrogen," *Science*, vol. 339, p. 417, 2013.

[56] Jaeckel J. and Roy S., "Spectroscopy as a test of Coulomb's law: A Probe of the hidden sector," *Phys. Rev.*, vol. D82, p. 125020, 2010.

[57] Barlow R., "Systematic errors: Facts and fictions," in *Advanced Statistical Techniques in Particle Physics. Proceedings, Durham, UK, March 18-22, 2002*, pp. 134–144, 2002.

[58] Stump D., Pumplin J., Brock R., Casey D., Huston J., Kalk J., Lai H. L., and Tung W. K., "Uncertainties of predictions from parton distribution functions. 1. The Lagrange multiplier method," *Phys. Rev.*, vol. D65, p. 014012, 2001.

[59] Pachucki K., "Theory of the Lamb shift in muonic hydrogen," *Phys. Rev. A*, vol. A53, p. 2092, 1996.